

A
DISSERTATION REPORT
ON

“Gold nanoparticle uptake in polymersomes for bio-medical applications”

Submitted for partial fulfillment of the requirement for award of the degree of

MASTER OF TECHNOLOGY
IN
Discipline (Polymer Science & Technology)

Submitted by

Shruti Pattanaik

09120059

UNDER THE GUIDANCE OF

Prof. Yuvraj Singh Negi

(Professor-in-Charge)

Department of Polymer & Process Engineering

IIT Roorkee, India

&
Dr. Dietmar Appelhans

(Head-Bioactive & Responsive Polymer Department)

Leibniz Institute for Polymer Research, Dresden, Germany



DEPARTMENT OF POLYMER & PROCESS ENGINEERING
INDIAN INSTITUTE OF TECHNOLOGY ROORKEE
SAHARANPUR CAMPUS
JUNE -2014

Acknowledgements

I am deeply indebted to Dr. Dietmar Appelhans, my external supervisor for giving me this unique opportunity to work with his research group at the Leibniz Institute for Polymer Research, IPF Dresden. His constant guidance was integral in building the foundation of my conceptual understanding of a completely new topic for me. The discussions with him during our frequent meetings helped to create a solid framework for this thesis.

I would like to extend my sincere thanks to Prof. Dr. Y.S. Negi, who kindly agreed to be my supervisor at IIT Roorkee and allowed me to undertake my dissertation studies abroad. He has played an immense role by always motivating me to pursue research in the field of polymer science. His constant encouragement and endless patience during the whole of my student career is deeply appreciated.

I would also like to thank my colleague Ms. Banu Iyisan at IPF for synthesising and supplying me with the polymers. Throughout this project, she supported me not only academically but also by being a great mentor. I would like to extend my thanks to Dr. Ulrich Oertel for the enlightening discussions on plasmon behaviour. Dr. Peter Formanek and Dr. Georgi Stoychev have my heartfelt thanks for providing me with the Cryo-TEM analysis that was so vital for this thesis.

I would like to thank my family who have always been supportive of all my decisions and encouraged me to aim higher. I also thank my friends for their constant affection and emotional support.

Shruti Pattanaik

Date: Jun 2, 2014

Name of Student: Shruti Pattanaik

CANDIDATE'S DECLARATION

I hereby declared that the work which is being presented in this Dissertation Report entitled "Gold nanoparticles uptake in polymersomes for bio-medical applications" in partial fulfillment of the requirement for the award of the degree of Integrated Master of Technology in Polymer Science and Technology, IIT Roorkee is a record of my own work carried out, under the supervision of Prof. Dr. Y.S. Negi, Department of Polymer and Process Technology, IIT Roorkee and Dr. Dietmar Appelhans, Leibniz Institute of Polymer Research Dresden.

The matter embodied in this project report has not been submitted by me for the award of any other degree.

Date: 02.06.2014


Place: Dresden, Germany


Shruti Pattanaik

Shruti Pattanaik

Student's Name

This is to certify that the above statement made by the candidate is correct to the best of our knowledge.


Internal Supervisor *Y.S. Negi*


Leibniz-Institut für Polymerforschung
Dresden
Hohe Straße 6
01069 Dresden

External Supervisor

Dr. Dietmar Appelhans

Table of Contents

List of Abbreviations	9
Abstract	11
1. Introduction	12
2. Theoretical background	14
2.1 Gold nanoparticles	14
2.1.1 Optical properties of AuNPs	15
2.1.2 Uses of AuNPs in bio-medicine	17
2.1.3 Challenges of using gold nanoparticles in bio-medicine	20
2.2 Polymersomes	21
2.2.1 Polymersomes – Basic introduction	21
2.2.2 Polymersome preparation methods	23
2.2.3 Polymersome morphology and self assembly mechanism	24
2.2.4 Stimuli responsive polymersomes	26
2.2.5 pH responsive polymersomes	26
2.3 Gold nanoparticles uptake in polymersomes	28
2.3.1 In-situ formation and encapsulation of gold nanoparticles	29
2.3.2 Incorporation of gold nanoparticles during self-assembly process	30
2.3.3 Challenges faced during nanoparticles incorporation in polymersomes	31
2.4 Specific recognition interactions	32
2.4.1 PEG – PEG interchain digitation	33
2.4.2 Threading interactions between Polyethylene glycol and Cyclodextrin	34
2.4.3 Adamantane – β - Cyclodextrin host-guest complexation	36
3 Experimental Section	39
3.1 Polymersome preparation	39
3.2 Direct encapsulation of gold nanoparticles in polymersomes	40
3.2.1 Preliminary trial encapsulation for 12 nm gold nanoparticles	40
3.2.2 Encapsulation of 30 nm citrate stabilised gold nanoparticles	42
3.2.3 Encapsulation of 60 nm citrate stabilised gold nanoparticles	43
3.3 PEG-AuNP hybrid interactions	43
3.4 Threading interaction between PEG and β -cyclodextrin	45
3.5 Gold nanoparticle uptake in polymersomes using host-guest complexation	48
3.6 Characterisation techniques and instrumentation	49
3.6.1 Dynamic light scattering	49
3.6.2 UV-vis spectroscopy	50

3.6.3	TEM measurements	50
3.6.4	UV irradiation.....	50
3.6.5	Hollow fibre filtration	51
4	Results and discussions	52
4.1	Polymersome formation.....	52
4.1.1	Dynamic light scattering results	52
4.2	Direct encapsulation of gold nanoparticles in Polymersomes.....	53
4.2.1	Encapsulation for 12 nm gold nanoparticles	53
4.2.1.1	Dynamic light scattering results	53
4.2.1.2	UV-vis spectroscopy results.....	55
4.2.2	Encapsulation for 30 nm gold nanoparticles	56
4.2.2.1	Dynamic light scattering results	56
4.2.2.2	Cryo TEM results	58
4.2.3	Encapsulation for 60 nm gold nanoparticles	60
4.2.3.1	Dynamic light scattering results	60
4.2.3.2	Cryo TEM results	61
4.3	Gold nanoparticle uptake by PEG - AuNP hybrid.....	63
4.3.1	Surface modification of 60 nm AuNP with thiolated PEGs	63
4.3.1.1	UV-vis spectroscopy results.....	63
4.3.1.2	Dynamic Light Scattering results	65
4.3.1.3	TEM Analysis.....	65
4.3.2	Gold nanoparticle uptake by PEG-AuNP hybrid.....	67
4.3.2.1	UV-vis spectroscopy results.....	67
4.3.2.2	Dynamic Light Scattering Results	69
4.3.2.3	Cryo TEM results	70
4.4	Threading interaction between BCD-PEG.....	71
4.4.1	Surface modification of 60 nm AuNP with β -cyclodextrin ligands.....	71
4.4.1.1	UV-vis spectroscopy results	71
4.4.1.2	Dynamic Light Scattering results	74
4.4.2	Gold nanoparticle uptake by threading interaction between BCD-PEG.....	74
4.4.2.1	UV-vis spectroscopic results	74
4.4.2.2	Dynamic Light Scattering results	76
4.4.2.3	Cryo TEM results	77
4.5	Gold nanoparticles uptake using host guest chemistry	79
4.5.1	UV-vis spectroscopic results	80

4.5.2	Dynamic Light Scattering results	82
4.5.3	Cryo-TEM results	83
5	Conclusion	86
	References	89
	Corrigendum	95



List of Abbreviations

AuNP	Gold nanoparticle
DLS	Dynamic Light Scattering
UV-vis	Ultra Violet-visible
nm	nanometre
Cryo-TEM	Cryogenic Transmission Electron Microscopy
PEG	Polyethyleneglycol
SPR	Surface Plasmon Resonance
LSPR	Localised Surface Plasmon Resonance
NIR	Near Infrared Region
SERS	Surface Enhanced Resonance Scattering
DNA	Deoxyribonucleic acid
MPS	Mononuclear Phagocytic System
siRNA	Small interfering RNA
EGFR	Epidermal Growth Factor Receptor
CTAB	Cetyl trimethylammonium bromide
CMC	Critical Micellar Concentration
p	Packing factor
NIPAM	N-isopropylacrylamide
LCST	Lower Critical Solution Temperature
PAMPA	poly[N-(3-aminopropyl)-methacrylamide]
PAA	poly(acrylic acid)
PS	polystyrene
P4VP	poly(4-vinyl pyridine)
PEO	poly(ethylene oxide)
DEA	(diethylamino)ethyl
TMSPMA	(trimethoxysilyl)propyl methacrylate
THF	tetrahydrofuran
PDEAEM	poly(diethylaminoethyl methacrylate)
PEI	Polyethylenimine
Mal	Maltose
BMA	Methylacryloyloxy benzophenone
PMPC	poly - [2-(methacryloyloxy) ethylphosphorylcholine]

PDPA	poly - [2-(diisopropylamino) ethyl methacrylate]
D_0	diameter of the gold nanoparticle
dw_0	vesicle wall thickness
RAFT	Reversible Addition-Fragmentation chain Transfer
Å	Angstrom
M	Molar
mg	milligram
mL	millilitre
NaOH	Sodium Hydroxide
HCl	Hydrochloric acid
μm	micrometre
BCP	Block copolymer
HF	Hollow Fibre Filtration
MWCO	Molecular Weight Cut-Off
kDa	kilo Dalton
β -CD	β -Cyclodextrin
mM	milliMolar
Ada	Adamantane
Wt%	Weight%
rpm	rotations per minute
λ	wavelength
keV	kilo electron voltage
TMP	trans-membrane pressure
PDI	Polydispersity index
avg	average
λ_{max}	Wavelength corresponding to maximum absorbance peak
NA	Not Applicable
CDexB053	Heptakis-(6-amino-6-deoxy)- β -cyclodextrin
CDexB013	6-Monodeoxy-6-monoamino- β -cyclodextrin

Abstract

This thesis focusses on the investigating a suitable route to enable uptake of large sized (30 nm and 60 nm) gold nanoparticles by pH responsive polymersomes of diameters ranging from 110-140 nm. Addition of these gold nanoparticles(AuNP) during self-assembly process of polymersomes, was found to have poor encapsulation efficiency after investigations by DLS, UV-vis and Cryo-TEM. Moreover, a significant size reduction was observed in case of encapsulated samples. Specific interactions like inter-chain digitation, threading interactions and host-guest complexation were employed to improve AuNP uptake by polymersomes. However, formation of PEG-AuNP hybrid due to interchain digitation by PEG was unsuccessful. But, investigations with β -Cyclodextrin modified AuNP showed a possibility for their uptake by threading complexation with PEG chains of polymersomes. Lastly, successful uptake of large sized AuNPs by polymersomes was achieved by host-guest complexation between β -Cyclodextrin immobilised on AuNP and Adamantane moieties on the polymersome.

1. Introduction

Although gold has held a fascination for mankind since its discovery, it is only in the last few decades with the aid of quantum leaps made in the field of nanotechnology that gold nanoparticles have found tremendous applications in the field of biomedicine (1). Gold nanoparticles possess unique size dependent optical properties like surface plasmon resonance and second harmonic generation, along with versatile chemical properties like inertness, thermal stability and easy functionalisation ability (2). These interesting properties have enabled the use of gold nanoparticles in biomedical applications for imaging purposes as diagnostic tools as well as for therapeutic uses by drug and gene delivery vehicles (3). However, the aggregation tendency of the gold nanoparticles along with the small sized nanoparticles currently used for bio-medical applications severely limit them from attaining their maximum potential as bio-medical agents. To alleviate these obstacles in the path of the use of gold nanoparticles in biomedicine, researchers have incorporated gold nanoparticles in polymer vesicles or polymersomes (4). Polymersomes are artificial vesicles which have better stability compared to their biological counterparts (5). Due to their unique structure of possessing both hydrophilic and hydrophobic entities on the same system along with an enclosed structure, they serve as an excellent template for nanoparticle uptake. But such gold nanoparticle encapsulation studies have been mostly carried out for gold nanoparticles ranging from 1-10 nm with polymersomes between 100-300 nm in size (6). Larger sized gold nanoparticles (beyond 20 nm) show enhanced optical properties and are therefore more attractive for bio-medical applications. However, uptake studies of such large gold nanoparticles in polymersomes have not attempted before due to the challengingly higher size ratio between the encapsulated nanoparticles and the encapsulating polymersome.

The aim of this thesis is to study the different possible routes by which successful uptake of large sized gold nanoparticles (30 nm and 60 nm) can be performed in pH responsive polymersomes of size ranging from 120-140 nm. Encapsulation of small sized gold nanoparticles (1-10 nm) is in itself an uphill task as reported by various researchers. Therefore, attempting to internalise even larger nanoparticles is a daunting prospect. But in order to successfully create a smart pH-responsive polymersome system with gold nanoparticles, complete encapsulation is not the only approach. Immobilisation of the gold nanoparticles on the surface of the

polymersomes is another viable alternative to synergistically combine the properties of both the polymersomes as the larger sized gold nanoparticles. Such an association with the polymersomes would screen the nanoparticles from each other and allow additional flexibility to functionalise the polymersomes for targeted bio-medical applications as a theranostic device functioning both as therapeutic agent in tandem with acting as a diagnostic tool.



2. Theoretical background

2.1 Gold nanoparticles

Colloidal sol of gold nanoparticles has held a centuries old fascination for the human mind, starting with the science of alchemy in the middle ages to its current omnipresent status in the field of bio-medicine. The first known extraction of gold started near a region in modern day Bulgaria in 5th millennium B.C. and spread thereafter towards the other civilizations like Egypt, China and India (3). It is here that the reference to colloidal gold can be found in tracts by the ancient Chinese, Arabic and Indian scientists. They called it the “gold solution” or “liquid gold” and used it particularly for medicinal purposes.

In the Middle ages in Europe, the alchemists aggressively looked for newer methods to synthesise this precious metal and developed potions to cure maladies. The alchemist Paracelsus writes extensively about the medicinal properties of this “potable gold”, which he prepared by reducing auric chloride with oil plant extracts or alcohol, to cure mental disorders and syphilis (7). Gradually, the fabulously curative powers of the colloidal gold extended to cures for heart and venereal problems, dysentery, epilepsy, tumors and going as far as being proclaimed as the “elixir for longevity”. In 1676, the German chemist Johann Kunckels published a book, concerning the “drinkable gold that contains metallic gold in a neutral, slightly pink solution that exert curative properties for several diseases” (3). In this he shared a remarkable insight that “gold must be present in such a degree of communitation that it is not visible to the human eye”. This is the known first reference to the effect of size of the gold particles and hereafter many such examples can be found of scientists in the 19th century striving to explain the vastly different coloured solutions of gold.

In 1857, Michael Faraday, reported the formation of deep red solutions of colloidal gold by reduction of an aqueous solution of chloroaurate (AuCl_4^-) using phosphorus in carbon disulphide or diethylether (8). After extensive investigations of the light scattering properties and turbidity of the colloidal sol, he concluded that the system was composed of tiny particles suspended in the aqueous phase which gave it the inherent colour. Moreover, he was of the opinion that the size of these colloidal gold

particles was smaller than the wavelength of visible light (9). Faraday provided the first result of the ability of the colloidal gold to stain organic tissues like gelatin and fabric (9). This important breakthrough is now the cornerstone of modern day spectroscopical techniques which make use of gold as an optical diagnostic tool.

In 1971, British researchers, W. P. Faulk and G. M. Taylor described a technique in which colloidal gold served as an immunochemical marker when it was conjugated with antibodies for direct electron microscopic visualization of Salmonella surface antigens (10). Examples of ground-breaking research such as this and others, shifted the focus of numerous biologists and chemists towards the potential uses of gold in bio-medicine.

Applications of gold nanoparticles are now widely ranging from diagnostics, genomics, targeted drug delivery, detection and photothermolysis of cancer cells to optical bio-imaging, etc. Such vast multitude of applications of AuNPs in bio-medicine can be attributed to its unique chemical and physical properties. As Faraday had demonstrated, the synthesis of the colloidal gold played a major role in influencing its size and hence, the subsequent properties determining its use in bio-medical applications. This has led to a spurt of research in the preparation of gold colloids by Schmid (11), Brust (12) and Turkevich et.al (13).

2.1.1 Optical properties of AuNPs

Gold nanoparticles are extremely interesting due to their significant optical properties, owing to their absorption and emission wavelengths lying in between the visible range. These optical properties are dependent on the size and shape of the gold nanoparticles which makes them uniquely suitable for various applications like diagnostic tools and bio-markers. Additionally, gold being a noble metal shows surface plasmon resonance (SPR) behavior unlike other nanoparticles such as polymeric nanoparticles, quantum dots, etc (1). Essential for surface plasmon resonance is the presence of free electrons on the interface of the two materials upon which light is incident. (1) (14). The electromagnetic wave excites the vibrational and electronic states of the metal particle when it passes through the particles. The free electrons are then set into a collective coherent oscillated state due to displacement, causing a charge separation with respect to the ionic lattice. Consequently, dipole

moments are created which then oscillate along the direction of the electromagnetic field and with the frequency of the incident light. This collective coherent oscillation of the free electrons is known as localized surface plasmon resonance (LSPR). The frequency at which the oscillation amplitude reaches a maximum is called the surface plasmon resonance (SPR). At this particular frequency, there is a strong dip in the reflection of the incident wave as it is strongly absorbed by the plasmon band of the excited metal nanoparticles (15). The SPR band intensity can thus be measured by UV-vis spectrometry. The optical response of the metal nanoparticles is dependent on their size, shape, interparticle distance, composition and properties of the local dielectric environment surrounding the nanoparticles (7) (15) (16). Consequently, a change in the intensity or the wavelength of maximum absorption can provide a good measure of the particle size, concentration, shape and dielectric properties (14). Gold, silver and copper nanoparticles show strong SPR bands in the visible region whereas other metals show broad and weak SPR bands in the UV region (17) (18). Although, silver nanoparticles induce better surface plasmon resonance behavior, gold nanoparticles are favoured because of their larger chemical inertness compared to silver nanoparticles (16).

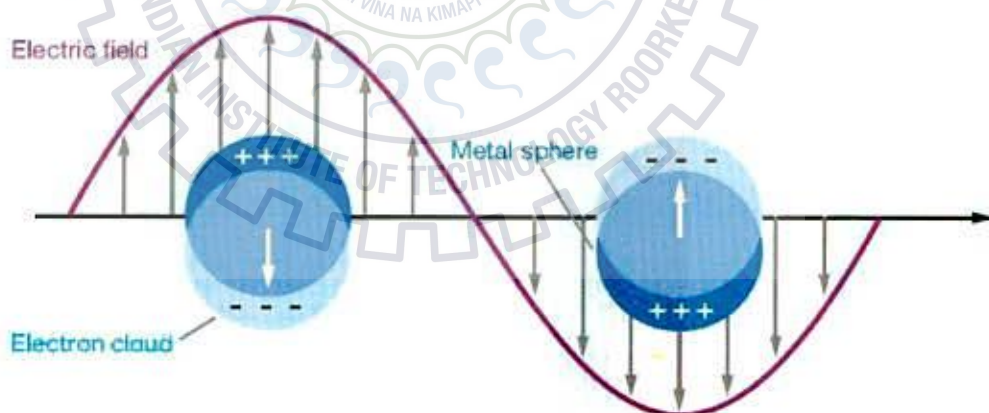


Figure 1: Schematic representation of surface plasmon resonance behavior of metal particle (19)

This surface plasmon resonance property is shown by spherical gold nanoparticles in the visible spectral region, giving the gold nanoparticles solution their vivid reddish colour. The colour of the gold nanoparticles solution changes with respect to the size of the nanoparticles. Nanospheres with a size of 20 nm in diameter show the reddish colour due to the large absorption of the incident light. Nanoparticles smaller than 10 nm in diameter have severely damped oscillations and therefore do not show a distinct

SPR band. Gold nanoparticles with sizes greater than this generally show surface plasmon band at 520 nm but even larger particles (80 nm), cause increased scattering of light take place corresponding to a broad shift in the surface plasmon resonance band which is also known as the red shift (19). Therefore, this shift in SPR band could be used an effective tool to understand the formation of aggregates of the gold nanoparticles when they are exposed to molecules bearing specific recognition sites or they can be used to determine the changes occurring on the surface of the nanoparticles by interacting ligands.

Another interesting inherent optical property of gold nanoparticles is the second harmonic generation. Second harmonic generation is the non-linear optical behaviour depicted by some materials that when they are irradiated by laser, photons double the energy of the incident light are generated. Materials which show this frequency doubling effect can be used as optical antennas to create increased absorption of laser light in localized areas. Therefore, optical antennas can be defined as materials which can convert an incident light wave into a localized field that would interact with the sample (20). The optical antenna can therefore be treated as a light source. In 1988, Ulrich Ch. Fischer and Dieter W. Pohl, successfully demonstrated that polystyrene coated gold particles (now referred to as gold nanoshells) can act as an effective localized light source (20) (21) (22).

2.1.2 Uses of AuNPs in bio-medicine

Gold nanoparticles have been used in medicinal preparations since their discovery. However in the recent years, bio-medical applications of metal nanoparticles in general and most specifically that of gold nanoparticles have reached dramatic proportions. This can be attributed to their unique properties of small size, large surface area to volume ratio, stability over high temperature, chemical inertness, inter-cellular diffusion capability and less cytotoxicity (2). Gold nanoparticles find uses as both therapeutic agents as well as diagnostic tools.

These remarkable properties of gold nanoparticles have led to its increased use in diagnostics in the shape of visualization and bio-imaging of various chemical and biological species (7). The strong light scattering property of gold nanoparticles coupled with their superior photo-stability has led to their use in imaging of cancer

cells (1). Moreover, the light absorption of biological specimens at near infrared region (NIR) is quite low and hence, gold nanoparticles are used as effective contrast agents for in-vivo imaging applications in either near infrared region (NIR) or for surface enhanced resonance scattering (SERS) (19). Additionally, nanoparticles can selectively accumulate in cancerous cells at higher concentrations than in ordinary cells (2). For development of more efficient imaging techniques, gold nanoparticles owing to their easy functionalisation are conjugated with suitable bio-markers (3) (19) (1). For example, gold nanoparticles conjugated with Bombesin peptides, are used for efficient imaging of cancer cells because of the preference of the gastrin releasing peptides (which are over-expressed in cancer cells) for these Bombesin peptides (2). All the above mentioned properties combined with good detection sensitivity enables their use in dark field, dual-photon luminescence microscopy as well as for fluorescence spectroscopy (19).

Apart from this, PEGylated hybrids, cell-specific peptide conjugates, DNA functionalized gold nanoparticles have found numerous applications such as dot immuno assays, immuno-chromatographic assays, immune-electron microscopy and plasmonic bio-sensors.

Another most important bio-medical application of gold nanoparticles is in the field of therapeutics. Good intracellular diffusion capability renders the gold nanoparticles as viable agents for targeted cellular applications. However, one of the major concerns which hinder their use is the ability of the gold nanoparticles to stay in circulation in the blood stream for sufficient time to release their drug load. There are two main clearance mechanisms by which nanoparticles can be rejected out of the body and thus leading to an inefficient drug carrier system. The first is by renal clearance during purification by kidney and the second is uptake by mononuclear phagocytic system (MPS) (23). For successful avoidance of renal clearance, the nanoparticles should be larger than 10 nm in diameter (24) and smaller than 500 nm to avoid recognition and uptake by MPS (25).

The easy surface functionalisation property of gold nanoparticles comes in aid to improve circulation time in the blood stream by reducing the clearance rate and augment the cellular internalization of the nanoparticles. PEGylation of gold nanoparticles has been widely reported as a method to improve bio-compatibility and

stability of nanoparticles, leading to prolonged blood stream circulation times (7) (23) (26) (2). But such immuno-repressive behavior induced by surface modification or functionalisation of the gold nanoparticles is largely dependent on the surface chemistry of individual hybrid systems and size of the particles and this consequently influences cellular internalization of the nanoparticles. Another important aspect to bear in mind is the toxicity Gold nanoparticles in therapeutics are mostly used as drug-carriers or gene-carriers and also for photo-thermal ablation therapy.

Gold nanoparticles functionalized with amino acids like glycine and lysine show better adherence to DNA and have been effectively used as gene-delivery carriers with less cytotoxicity (2). Additionally, the functionalized gold nanoparticles have been used as carriers for anti-sense nucleotides and therapeutic siRNA which are now being utilized in gene silencing therapies, due to their highly selective targeting mechanism (19) (27) (28). Likewise, peptide functionalized gold nanoparticles are being used for vaccine delivery because they can activate macrophages thereby exposing smaller molecules which were earlier undetectable (2).

Photo-thermal therapy of cancer cells using gold nanoparticles is another important medical breakthrough (2). The intense absorption behavior depicted by gold nanoparticles in the visible and near infrared region is instrumental in their use for this therapeutic procedure (1) (29). When irradiated with light either in the visible or infrared spectrum, the gold nanoparticles convert the absorbed light into heat by rapid phonon-phonon and electron-phonon processes (1). This causes localized heating and if the gold nanoparticles are located near the affected cells, then those cells are obliterated under the influence of this heating phenomenon. However, it is difficult Selective photo-thermal therapy has also been achieved by conjugating the gold nanoparticles with a chromophore or a biological marker which would enhance the internalization of the gold nanoparticles at a particular targeted cell location (7). Huang et. al. have shown that gold nanoparticles conjugated with anti-epidermal growth factor receptor antibodies (EGFR) selectively target the cancerous cells and can be used for effective in-vivo detection and decimation of these cells (1). Similarly, gold nanoparticles conjugated by fluorescent heparin are utilised for treatment of metastatic cancer cells (30). Other conjugates which have been used for targeted theranostic (therapeutic as well as diagnostic) applications are thiolated PEGs, peptides and folic acid.

2.1.3 Challenges of using gold nanoparticles in bio-medicine

In the previous sections, the extensive use of gold nanoparticles and its hybrid systems as both therapeutic and diagnostic tools have been explained. However, they also have certain disadvantages like cytotoxicity, aggregation tendency and issues with bio-compatibility which place limitations on their use as bio-medicinal agents.

As discussed previously, prolonged circulation time of gold nanoparticles in the blood stream is necessary for them to efficiently discharge their ability as diagnostic or therapeutic tools. However, presence of the nanoparticles in the cells for a too long and the inability of the body to excrete them out causes cellular damage and hence cytotoxicity. As size of the nanoparticles increases, renal clearance ability also decreases. However, gold nanoparticles up to a size of 200 nm can strike a balance between increased circulation time as well as effective excretion after a certain period of cellular internalization. Not only the size, but different capping agents and surface coatings also induce cellular cytotoxicity (31). CTAB capped gold nanorods have been adjudged to have as high as 80% cell deaths in HeLa cell assays. To counter the cytotoxic effects, PEG modified gold particles have been used which have showed reduced cytotoxicity by decreasing non-specific binding of the gold nanoparticles to the biological moieties (32).

Moreover, gold nanoparticles synthesized by the conventional reduction of the chloroauric ion solution by sodium borohydride are not very stable. Gold nanoparticles prepared by this are only stabilized by the ionic repulsions by the adsorbed AuCl_2^- ions. Gold nanoparticles already have a predilection to aggregate and in physiological conditions, when the gold nanoparticles are administered these surface charges are sufficiently screened to cause a loss in stability of the nanoparticles and induce agglomeration (33). Such aggregation tendency within the cellular membrane can lead to bio-accumulation and hence death of the healthy cells caused by the body's inability to flush out these large aggregates. Therefore, a lot of current research is focused on alternate methods to stabilize the gold nanoparticle systems. One of the most widely reported methods is the surface modification of the gold nanoparticles with polyethylene glycol chains. The PEG chains form monolayers on the gold nanoparticles surface and improve stability of the colloidal system due to the steric repulsions between the PEG chains (33).

Apart from the formation of such hybrid structure involving gold nanoparticles, researchers are now focused on encapsulating the gold nanoparticles in vesicular compartment like structures to address the problems of aggregation, cytotoxicity as well as improve cellular uptake. Foremost in this field of research is the incorporation of gold nanoparticles in polymersomes.

2.2 Polymersomes

Vesicles present inside the cellular structure are composed of a liquid enclosed within a lipid bilayer membrane. These vesicles can fuse with the cellular membrane and can carry external substances and discharge these contents inside the internal environment of the cell. Therefore, they are involved in numerous bodily functions like transport of materials, enzyme and protein storage, metabolism and also as biological nano-reactors. Owing to their multiple functionalities in biological processes, researchers have tried to create similar bio-mimetic structures known as liposomes and polymersomes (34). While liposomes are artificial vesicular structures composed of a lipid bilayer, polymersomes consist of artificially synthesized polymer membranes.

2.2.1 Polymersomes – Basic introduction

The bilayer membrane structure of liposomes consists of phosphatidylcholine-enriched amphiphilic phospholipids by which they derive their name (35). The liposomes consist of a hydrophilic liquid enclosed by hydrophobic membrane with hydrophilic external and internal coronas. Although such artificially engineered vesicles can be used to successfully mimic the bio-chemical reactions occurring inside the cells, they have numerous limitations. The most important being the stability of the membranes of these liposomes. Since, trans-membrane diffusion is one of these vital aspects which determine the functionality of such vesicular structures, scientists have tried to create similar vesicles but with better membrane properties. This has led to the synthesis of artificial amphiphilic di-block or tri block copolymers which can attain vesicle like structures. These amphiphiles form nano-sized hollow spheres called polymersomes, with a hydrophobic membrane and hydrophilic internal and external corona (5). The block copolymers consist of both hydrophobic and hydrophilic parts and tailoring the composition of the amphiphiles can be used to adjust the membrane

properties unlike those in the case of lipids. If the molecular weight of the hydrophobic block is higher, then a vesicular structure with a thicker membrane can be created. Moreover, polymers with higher overall molecular weight than lipids are used to obtain stronger and more robust polymersomes than the conventional liposomes (36). Additional membrane properties like permeability, mechanical stability and elasticity are also tunable in case of polymersomes (36) (37). In short, flexibility to design the blocks of the synthetic amphiphilic polymers imparts flexibility in design of the polymersome structure and its membrane (34). Due to such adjustability in its characteristics, polymersomes are at the forefront of research for potential uses in the fields of material science, bio-medicine and biology (38).



Figure 2: Schematic representation of a polymersome. Green & Gray colored chains indicate hydrophilic & hydrophobic parts of the block copolymer chain. Red coloured structures indicate the crosslinker.

The most exciting feature of polymersomes is the presence of both hydrophobic and hydrophilic functionalities on the same structure. This unique property has been used to encapsulate hydrophilic moieties in the hydrophilic interior cavity and embed hydrophobic molecules in the hydrophobic membrane of the polymersome. Additionally, the hydrophilic exterior of the polymersome can be used for functionalisation with other bio-molecules to improve their interaction with the surrounding medium in which they are dispersed (5). Therefore to describe a potential hybrid, dye-stained membrane can be used for tracking the movement of the polymersome, a targeting molecule conjugated on the surface will be used to home in on the affected cell and the therapeutic drug internalized in the corona can then be released for remedial action (36) (39) (40).

2.2.2 Polymersome preparation methods

In literature there are two generally reported methods for preparation of polymersomes by self-assembly of the chemically synthesised block copolymers. The first method is the solvent switch method, where the block copolymer is first dissolved using an organic solvent (41). Organic solvent is necessary because most of the block copolymers do not have good solubility in aqueous systems. The organic solvent should be selected bearing in mind that both the hydrophobic and hydrophilic blocks should be soluble in it. Upon complete dissolution of the block copolymer, water is added slowly to the system. As the water content increases, the hydrophobic block withdraws from the now poor solvent system and the hydrophilic block is increasingly solvated. At a critical micellar concentration (CMC), which itself is dependent on the type of the polymer, polymer molecular weight and the solvent, the block copolymer system self assembles to form micellar aggregates. Increasing water content gradually changes the morphology of the self assembled system through a series of structures ranging from spheres to rods and ultimately at a particular point into well defined polymersomes (41). Finally, the organic solvent is removed by dialysis which is a cumbersome and time-consuming process. Additionally, the morphology and the membrane of the polymersomes is altered due to changing solvent/water ratio during dialysis (5).

The second method is the film rehydration method which is also known as the organic solvent free method (5). However, essentially it is not a purely solvent free method because the initial dissolution of the block copolymer again involves an organic solvent like chloroform or tetrahydrofuran. But before the block copolymer self assembly process, the organic solvent is removed by evaporation to obtain a thin film of the block copolymer. The film so obtained is then rehydrated using pure water or an aqueous buffer. As in the case of solvent switch, the hydrophilic block is heavily solvated due to presence of water and self assembly process is triggered to generate polymersomes (42). This method of polymersome preparation is also known as film swelling. A similar method called bulk swelling is also employed for polymersome formation where the block copolymer is directly dissolved in water (5). As discussed previously, the copolymer is not well dissolved in an aqueous system therefore, the dissolution process is accompanied by vigorous agitation to aid in self assembly

process. However, such vigorous stirring inadvertently disturbs the self assembly process and leads to wide size distribution index of the formed polymersomes (43).

All the above mentioned methods for preparation of self assembled polymersomes systems are tedious, time consuming and economically less viable (44). Moreover, the polymersomes obtained by these protocols do not have stimuli responsive characteristics. Incorporation of stimuli responsive agents in polymersomes can increase their applications in bio-medicine as flexible therapeutic hybrids.

2.2.3 Polymersome morphology and self assembly mechanism

Amphiphilic block copolymers can attain a range of varied shapes and morphologies on self assembly. Most prominent among these are spherical micelles, rods, vesicles, disc like micelles, toroids etc. Likewise, polymersomes which are also broadly speaking artificial vesicles, can assume morphologically varied forms like simple vesicles, onion-like vesicles, multi-layer vesicles, tubular vesicles, flower-like vesicles and numerous other complex shapes (5).

The packing factor (p) is one method to determine the type of self-assembled morphology that a block copolymer will attain (45). It is defined by

$p = v/(al)$, where

v = volume of the hydrophobic block

a = interface area of a single molecule

l = hydrophobic length perpendicular to the interface

Table 1: Packing factor to determine vesicular shape

Range of packing factor	Morphological shape
$p \leq 1/3$	Sphere
$1/3 \leq p \leq 1/2$	Cylinder
$1/2 \leq p \leq 1$	Bilayer

Although factors like copolymer concentration, pH of the system, solvent/water ratio, type of solvent and temperature influence the morphology, the hydrophobic/hydrophilic block length ratio plays the key role in determining the final morphology (5) (41).

Table 2: Block copolymer characteristics influencing morphological shape

Hydrophobic:Hydrophilic ratio (x)	Morphological shape
$x > 1:1$	Micelles
$x < 1:2$	Vesicles
$x < 1:3$	Vesicles, inverted structures, complex aggregates

Likewise, polymersome size can be tuned by modifying the copolymer block lengths, solvent ratios and concentration of the polymers. Polymersome sizes generally range from 100 - 400 nm and their corresponding membrane thickness can vary from 5 nm to as high as 30 nm, depending on the block length ratio (46).

Polymersome formation mechanism is also of keen interest to researchers so that the self-assembly process can be controlled and tunable morphological structures obtained. It is generally assumed to be a two-step process wherein first the block copolymer forms a bilayer membrane which then rearranges to obtain a hollow closed structure (47). However, such a simplistic mechanism failed to explain the more complicated polymersome structure. Hence after numerous theoretical simulations which take into account the various molecular dynamics and Brownian dynamics, two models have been proposed. The mechanisms are represented in Fig. 3.

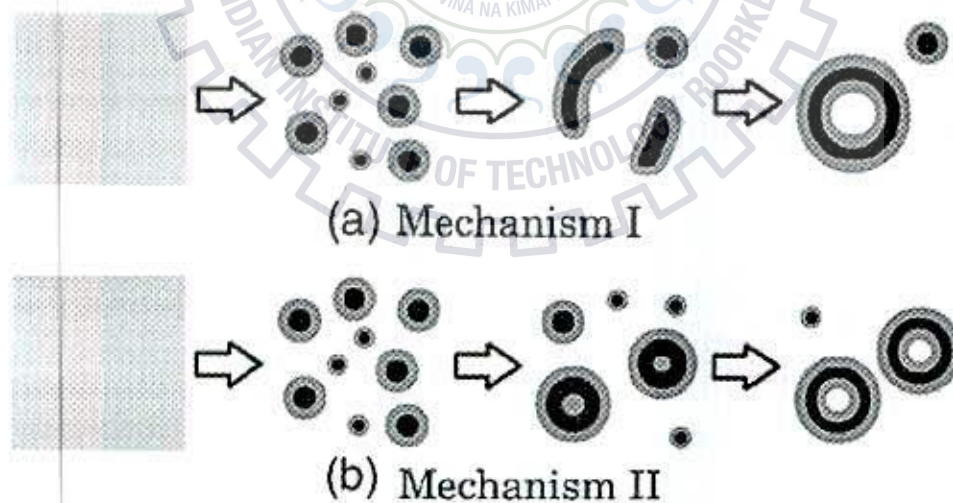


Figure 3: Mechanism for self-assembly process involving polymersome formation (48)

In mechanism I, at first small spherical micelles are formed which then create larger micelles by inter-micellar collision (48). These disc-like or cylindrical micelles subsequently form closed vesicular structures. Mechanism II forms the small micelles similar to the ones in mechanism I. But to form larger micelles, the smaller ones undergo an evaporation-condensation process. This is followed by solvent uptake into the interior of the large micelles to result in the final polymersome or vesicle.

2.2.4 Stimuli responsive polymersomes

To effectively function as miniaturized bio-medical devices and broaden the scope of their use, it is imperative that stimuli responsive polymersomes are created. Drug loading ability of polymersomes has already been discussed in previous sections. The polymersomes that we have discussed until now can only release their payload by diffusion that is not highly controllable. However, if the drug loaded polymersome undergoes spontaneous self-assembly triggered by external stimuli, then the efficacy of such therapeutic devices is largely enhanced.

In this light, several smart polymersomes, which respond to a variety of stimuli like light, pH, temperature, reduction/oxidation have been extensively studied (5). Light responsive polymersomes, incorporate a light sensitive moiety (chromophore) like azobenzene in the copolymer backbone. On UV-irradiation this chromophore induces trans \leftrightarrow cis conformations in the vesicle causing morphological changes (49).

Thermo-responsive polymersomes operate on the principle of changing hydrophilicity or hydrophobicity of the block copolymer component units, under the influence of altering temperature (5). The most widely used thermo responsive agent is N-isopropylacrylamide (NIPAM), which is soluble in aqueous systems below its lower critical solution temperature (LCST) of 32°C and is rendered insoluble in higher temperatures. Li et.al. prepared thermo-responsive polymersomes utilising this property of NIPAM with the copolymer system of poly[N-(3-aminopropyl)-methacrylamide hydrochloride]-b-PNIPAM(PAMPA-b-PNIPAM) (50).

But the status of the most important class of smart or stimuli responsive polymersomes is attributed to pH responsive polymersome, which will also serve as the system for this study. A detailed description of this category is undertaken in the following section.

2.2.5 pH responsive polymersomes

The human body hosts a wide range of pH environments like the pH of blood is 7.4, our digestive tract has a pH gradient from 1 to 7.5. Such a broad spectrum of physiological environments has attracted the attention of scientists to develop bio-

medical devices whose pH can be programmed to match that of the target organ. pH responsive polymersomes which are extensively used as drug delivery agents have therefore been keenly investigated for pH tunable characteristics. The underlying concept is to incorporate a pH responsive functional group like a weak base or a weak acid which can be protonated or de-protonated at differing pH, in the block copolymer (5).

Liu et.al. reported the first occurrence of pH triggered inversion of polymersomes formed by triblock, poly(acrylic acid)-b-polystyrene-b-poly(4-vinyl pyridine)(PAA₂₆-b-PS₈₉₀-b-P4VP₄₀) in DMF/THF/H₂O mixtures (51). In their investigation, at acidic pH of 1, the polymer vesicle was stable when the P4VP chains were on the outside and PAA chains on the inside, due to repulsive interactions. However, in an alkaline pH of 14, the PAA chains due to larger steric repulsions, switched to form the external layer of the polymersome with the P4VP chains in the interior of the polymersome.

In 2005, Du and Armes, reported a class of polymersomes with pH tunable membrane properties along with shape persistent characteristics (52). The pH sensitive polymersomes were formed by self assembly of poly(ethylene oxide)-b-poly[2-(diethylamino)ethyl methacrylate-*s*-3-(trimethoxysilyl)propyl methacrylate],[PEO-bP(DEA-*s*-TMSPMA)], in THF/water mixtures. The tertiary amino group in the PDEA unit at deprotonated at alkaline pH and was insoluble. Deprotonation closed the membrane pores reducing the membrane wall thickness as well as permeability. Subsequent protonation caused swelling of the vesicles, thereby imparting pH tunable membrane permeability. Shape persistence was conferred due to the cross-linking by self-catalysis avoiding dissociation of the vesicular structure at acidic pH.

In 2011, Voit et.al. reported the formation of photo-crosslinkable pH sensitive polymersomes using the block copolymer PEG₄₅-b-PDEAEM-*s*-PDMIEM structure (37). After dissolving the block copolymer in acidic solution, the polymersome structure formation was initiated by increasing the pH to deprotonate the tertiary amino group of PDEAEM. Crosslinking under UV irradiation and subsequent investigation of polymersomes under varying pH conditions by DLS proved the formation of stable, robust polymersomes with hydrodynamic diameter of 100 nm(at pH=9) which increased at lower pH. Uptake studies with hydrophobic and hydrophilic dyes were carried out to prove pH triggered entrapment as well release of the dye

molecule. PEI-Mal The same group investigated pH swelling behaviour of photo-crosslinked polymersomes and the cytotoxicity of such systems via cellular uptake studies and their potential uses as bio-nanoreactors (34) (53).

The efficiency of vesicular drug carrier was also investigated based on (PEG-b-P(DEAEMA-stat-BMA)) photo-crosslinkable and pH sensitive structure (54). This class of photo-crosslinkable polymersomes were stable over multiple pH switching cycles even with shorter cross-linking times. Successful investigation of pH dependent Doxorubicin uptake, retention and release mechanism soundly established that photo-crosslinked polymersomes could also used as tunable nano-carriers dependent on pH, crosslinking time and shear rate.

In light of these advances in the field of pH responsive polymersomes, it can be concluded that successful encapsulation of nanoparticles in polymersomes can be carried out. As discussed in the previous sections, gold nanoparticles due to their unfortunate tendency of agglomeration have limited bio-medical applications. Therefore, it was conceived that incorporation of gold nanoparticles in polymersomes, would provide an excellent solution to this problem. Additionally, the presence of PEG moiety would provide biocompatibility as well as increase circulation time in the blood stream due to the large size of the polymersomes (100-200 nm). Due to these lucrative advantages, gold nanoparticles incorporation in polymersomes is a separate and extensive field in itself.

2.3 Gold nanoparticles uptake in polymersomes

Nanoparticle incorporation in artificially designed nanocarriers finds extensive applications in catalysis, drug delivery, bio-sensor devices, etc (55). Polymersomes owing to their robust nature and unique property of having both hydrophilic and hydrophobic regions serve as perfect hosts for these nanoparticles. There are two different approaches reported in literature for incorporation of such nanoparticles in polymersomes which are discussed in the following sections.

2.3.1 In-situ formation and encapsulation of gold nanoparticles

The first approach involves the use of the polymer vesicle as a reaction compartment for formation of the gold nanoparticles. Polymersomes are formed wither using film rehydration technique or solvent switch method. The metal salt that is HAuCl_4 , is then solubilised within the hydrophobic membrane of the polymersome (56). Ion-exchange technology is sometimes employed to ensure the formation of the nanoparticles inside the polymersome (57). Reduction is carried out by introducing sodium borohydride and gold nanoparticles are formed within the polymersome.

In 2005, Du et.al formed pH sensitive photo-crosslinkable polymersomes by self-assembly of poly - [2-(methacryloyloxy) ethylphosphorylcholine] – block – poly - [2-(diisopropylamino) ethyl methacrylate] (PMPC-b-PDPA) in purely aqueous solution (58). Addition of HAuCl_4 solution protonated the amino group and the AuCl_4^- ions were incorporated in the membrane as counter ions. In-situ reduction produced gold nanoparticles of ~4nm embedded in the polymersome membrane.

This method can only be used for incorporation of gold nanoparticles within the hydrophobic membrane. This is mostly because the gold nanoparticles are by nature hydrophobic and since the membrane itself is hydrophobic, the nanoparticles are selectively embedded in the membrane wall. Moreover, the stability of the polymersome membrane is greatly reduced thereby limiting the potential applications of this hybrid structure. There is also lesser control over the growth and morphology of the in-situ prepared gold nanoparticles (59) (60).

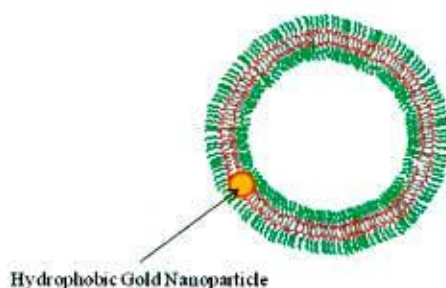


Figure 4: Schematic of AuNP embedded in polymersome membrane

GRS

2.3.2 Incorporation of gold nanoparticles during self-assembly process

This incorporation method is more versatile than the previous one. In this method, the gold nanoparticles are introduced into the system during the self assembly process of polymersome formation (59). Gold nanoparticles used in this approach are invariably pre-formed. This provides an added advantage of modifying the hydrophobic AuNP surface with hydrophilic capping agents like citrate, etc. to produce hydrophilic AuNPs which can then be guided selectively even into the hydrophilic corona of the polymersomes.

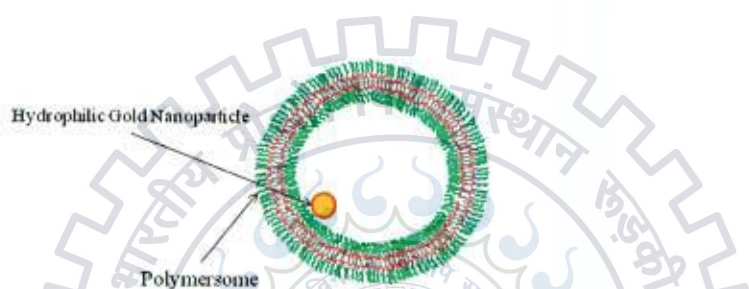


Figure 5: Schematic of AuNP internalised within the hydrophilic polymersome cavity

In 2007, Sachsenhofer et.al, produced AuNPs by Brust-Schiffin method and mixed them with a stock solution of PEO₃₀-PBD₄₆ copolymer followed by solvent evaporation (61). The hybrid film generated was then rehydrated forming multi-lamellar polymersomes embedded with AuNPs. The nanoparticles were again embedded in the hydrophobic membrane and no occurrence of partial inclusion of the nanoparticles was reported. The resultant polymersomes had a hydrodynamic size varying from 300 - 400 nm.

For the purpose of this study, we require to incorporate sufficiently larger sized AuNPs than previously reported in literature. Since, the thickness of the membrane wall varies from 5-30 nm as reported in literature, in-situ reduction and incorporation of gold nanoparticles within the membrane wall is impossible. Hence, incorporation of the nanoparticles will be performed during the self-assembly process. Consequently, it is imperative to understand the interfacial interactions as well as the influence of the nanoparticles during the self-assembly process.

2.3.3 Challenges faced during nanoparticles incorporation in polymersomes

Successful encapsulation of nanoparticles although has been widely reported, the process causes a destabilisation of the membrane, either by curving the membrane or by causing secondary interactions like budding and fission of the vesicles (59) (62).

Binder and co-workers produced significant results involving interfacial interaction effects of nanoparticle with vesicular membrane by making comparative encapsulation studies involving hydrophobic AuNP(2 nm), hydrophilic AuNP(12 nm) and hydrophilic retrovirus (30 nm) (56). Their studies concluded that hydrophobic AuNPs were localised in the vesicular membrane whereas hydrophilic AuNP accompanied by a size reduction of the polymersomes. However, they found that in the case of hydrophilic gold nanoparticles were evenly distributed on either side of the membrane structure. The vesicles so formed consisted of weak membranes and were more inhibiting in nature. The larger retrovirus particles which were also hydrophilic, formed stable vesicles but with budding effects upon encapsulation, indicating that larger particles in large concentrations may not be detrimental to polymersome structure. Therefore, our theoretical basis of encapsulating larger sized (50-70 nm) hydrophilic AuNPs inside the hydrophilic chamber of the polymersome is supported by this.

As discussed previously, the goal of this study is to incorporate large sized gold nanoparticles inside the polymersomes. Most of the AuNP uptake studies reported in literature have been carried out for AuNP size dimension between the range of 2-10 nm. To get a clear perspective of the location of encapsulated AuNP in polymersomes, Xu. et. al. performed extensive size dependent studies involving gold nanoparticle uptake (63). In this study, AuNPs were coated with hydrophobic 1-dodecanethiol by ligand exchange or Polystyrene to provide colloidal stability. According to their enthalpic and entropic calculations, gold nanoparticle uptake was found to be size dependent. They concluded that the ratio of the diameter of the AuNPs (D_0) to the vesicle wall thickness (dw_0) was an important parameter to determine the location of AuNP in the spherical vesicle. A D_0/dw_0 ratio greater than 0.5 was found to result in expulsion of the AuNP from the vesicle wall and its subsequent relocation in the interior of the micelle. Such an arrangement led to the formation of an energetically and entropically favourable system.

Citrate stabilised AuNPs with sizes of 30 and 60 nm will be utilised for this study. The size of our polymersome will be about 120-140 nm with a vesicle wall thickness of 20 nm. Therefore there would be two factors responsible for guiding the location of the used AuNPs in the polymersome. The first is the hydrophilic nature of the AuNPs, which will encourage the nanoparticles to form favourable interactions with the hydrophilic core of the polymersome. The second and more important factor will be the size ratio of the AuNPs and the vesicle wall. As demonstrated by Xu et.al, the proposed AuNPs exceed the D_0/dw_0 ratio by a factor of 3, and hence to form an energetically stable polymersome structure, again the polymersome cavity will be the preferred location.

In spite of these two strong motivating factors there might be another very real possibility that the size of these AuNPs will prove too large for even the polymersome cavity to accommodate within itself. Some studies have suggested that the volume fraction of the incorporated nanoparticles might affect the nanoparticles-polymersome hybrid system, although no mathematical models have been created to quantitatively determine this. But it might also be logical to postulate that the polymer chains of the vesicle may not be able to endure a greater degree of chain stretching if there are to encapsulate such a large particle. In the possibility of such an event, there arises a need to have additional specific interactions between the polymersome and the incoming gold nanoparticles to improve its chances of incorporation.

2.4 Specific recognition interactions

When dealing with complex hybrid systems like the one that we have now in this study, that is gold nanoparticles incorporation in polymersomes, it is always necessary to control the morphology of the hybrid. As discussed in the previous section, the comparatively large size of the AuNPs might prove detrimental to their chances of encapsulation within the polymersome. Therefore, it might be prudent to introduce moieties bearing specific recognition capabilities to selectively guide the gold nanoparticles to a pre-determined location in the polymersome system. Supramolecular chemistry with its vast array of non-covalent interactions like hydrogen bonding, host-guest interaction, electrostatic interactions, etc. provides ample choices to select the best guiding influences.

2.4.1 PEG – PEG interchain digitation

Surface coatings consisting of biopolymers or synthetic macromolecules have been used for modification of the gold nanoparticles in order to impart them specific recognition behaviour and assist in the self-assembly process (64). One of the most common methods employed is the grafting of macromolecular ligands on the AuNP surface to create hybrid amphiphiles. To achieve these complex structures, three routes namely; ligand exchange, grafting to and grafting from methods have been reported in literature (65). Zhao et. al. grafted Polystyrene on gold nanoparticles to obtain organic-inorganic hybrid particles. Thiol terminated hydrophilic poly(N-vinylpyrrolidone) (PVP-SH) was synthesised by RAFT polymerization and added to the hybrid nanoparticles mixture in an organic solvent. The amphiphiles on dissolution in an aqueous medium, quickly self-assembled to protect the hydrophobic polystyrene with the hydrophilic AuNPs internalised in the corona and PVP chains forming the exterior of the vesicle (65).

A similar approach involving grafting of polyethylene chains on the surface of gold nanoparticles will be adopted in this study. This is easily done because citrate stabilised gold nanoparticles can be readily modified by thiol terminated molecules or polymers (65). Grafting of PEG chains imparts hydrophilic character to the gold nanoparticles. Additionally, the stability of the gold nanoparticles is improved due to the steric repulsions between the grafted PEG chains (66). It is proposed that the PEG chains grafted on the AuNPs will interact with the those on the pH responsive block copolymer PEG₄₅-b-P(DEAEMA-stat-BMA) used for polymersome formation to form a PEG-AuNP hybrid. The PEG-PEG interactions might be due to thermodynamic factors induced by similar miscibility, or there might also be physical entanglements caused by intermolecular chain digitations during the self-assembly process. Moreover, the hydrophilic nature of the PEG grafted AuNP might preferentially guide it to locate in the hydrophilic corona of the polymersome.

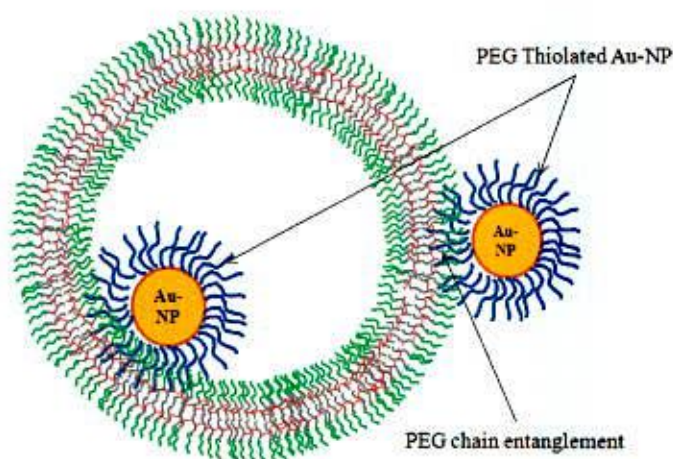


Figure 6: AuNP uptake by polymersome due to PEG-AuNP hybrid formation

2.4.2 Threading interactions between Polyethylene glycol and Cyclodextrin

Research on molecular recognition systems have been mostly focussed on low molecular weight entities (67). However, it is also possible to obtain such specific recognition abilities even in case of large macromolecules. Cyclodextrins are at the centre of such interesting supramolecular systems. Cyclodextrins are water soluble oligosaccharides formed by glucopyranose units linked together in a ring like structure (68). β -Cyclodextrin is such a molecule that has 7 glucose units which form a three-dimensional toroidal structure with a hydrophobic cavity. The cavity serves as a host to low molecular weight polyethylene glycols and forms an inclusion complex (67). It was shown by Harada that this complexation process was dependent on the relationship between the cross-sectional areas of the cyclodextrin cavity and the guest macromolecule. Two PEG chains penetrated the α -Cyclodextrin cavity to form a tight fit and precipitated due to the formation of the complex. Furthermore, it was suggested that neighbouring α -Cyclodextrins threaded themselves in head-to-head or tail-to-tail configurations to form unique structures called rotaxanes. .

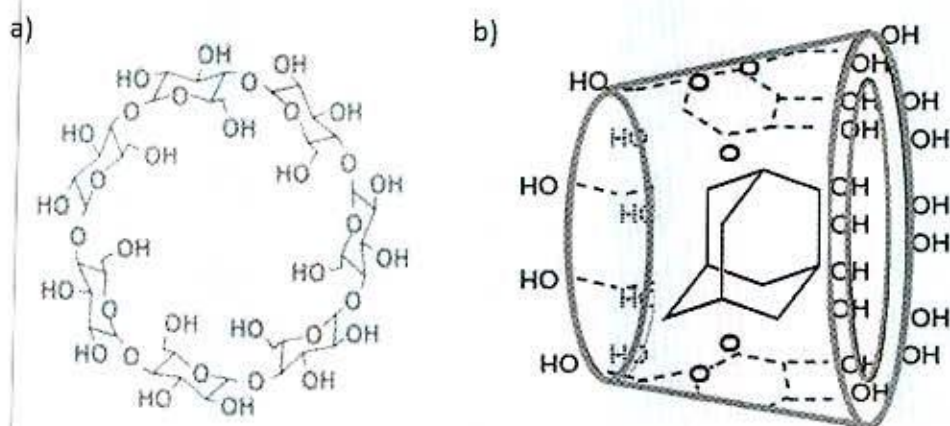


Figure 7: a) Chemical Structure of β -Cyclodextrin

b) Schematic for adamantane - β -Cyclodextrin host guest complexation mechanism. Adamantane perfectly fits into the β -Cyclodextrin cavity.

Interestingly, rotaxane formation between α -Cyclodextrin and polyethyleneglycol chains have been utilised to initiate self-assembly process in case of block copolymer for polymersome formation. Jiet, al. introduced α -Cyclodextrin to the block copolymer system of poly(ethylene oxide)-b-poly(2-methacryloyloxyethyl phosphorylcholine) (PEO-b-PMPC) in aqueous media (69). Rotaxane formation triggered the self-assembly process resulting in polymersomes between 100-200nm.

Although α -Cyclodextrins form these complexes with many macromolecules including PEG, β -Cyclodextrins have not been so prolific. This is mainly attributed to the fact that β -Cyclodextrin has a larger cavity than α -Cyclodextrin and therefore, the macromolecular chains do not fit snugly its cavity. However, investigations about possible formation of such complexes with higher molecular weight PEG have not been performed.

Therefore, β -Cyclodextrin grafted AuNPs will be introduced to the block copolymer system containing PEG chains and investigation of possible inclusion complexation and its influence as a guiding ligand will be carried out within the scope of this study.

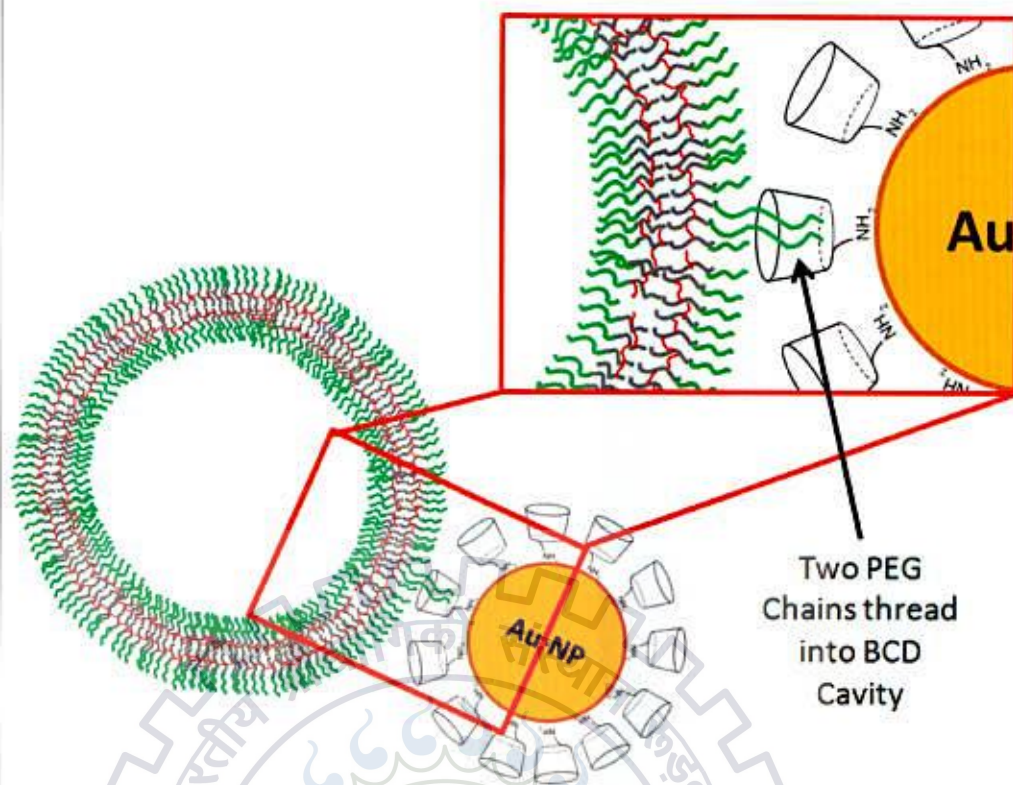


Figure 8: AuNP uptake by polymersome due to PEG- β -cyclodextrin threading interaction

2.4.3 Adamantane – β - Cyclodextrin host-guest complexation

One of most important interactions in supramolecular chemistry is the host-guest complexation mechanism. In such complexes, two or more entities are bound together by non-covalent forces to form a concerted system. Due to this, the supramolecular hybrids are not as strong as covalently bonded systems, but the association constant provides a means to gauge the stability of the system. The larger molecule is generally referred to as the host with the smaller molecule becoming the guest.

β -Cyclodextrin has external surface is highly hydrophilic due to the presence of hydrophilic groups and it has a hollow hydrophobic cavity which serves a host for other hydrophobic moieties (70). Adamantane (tricyclo[3.3.1.1(3,7)]decane, $C_{10}H_{16}$) is a crystalline compound with an arm-chair like conformation formed by the fusion of four cyclohexanes (68). The highly hydrophobic nature of adamantyl moiety along with its diameter of 7 Å fits tightly into the β -Cyclodextrin cavity to form a strong inclusion complex. This host-guest complex is highly stable with an association constant of 10^4 – $10^5 M^{-1}$. Therefore, this supramolecular complex has found extensive

applications in hydrogels, drug-delivery carriers, cyclodextrin based polymer systems, and bio-sensors etc.

Ritter et.al.reported the formation of tubular vesicles by host-guest interactions between β -Cyclodextrin and adamantane modified poly(ethylene imine) PEI (71). The morphologies of these structures were similar to that of liposomes and the vesicles were stable over a range of pH. Ha et.al. used a similar mixed polymer approach to form Adamantyl- β -Cyclodextrin host guest complexation induced vesicles (72). They produced cyclodextrin capped AuNPs which were complexed with Ada-terminated PNIPAM/PEG which formed amphiphilic AuNPs. At a temperature lower than the LCST of PNIPAM, the amphiphiles self assembled into vesicular structures.

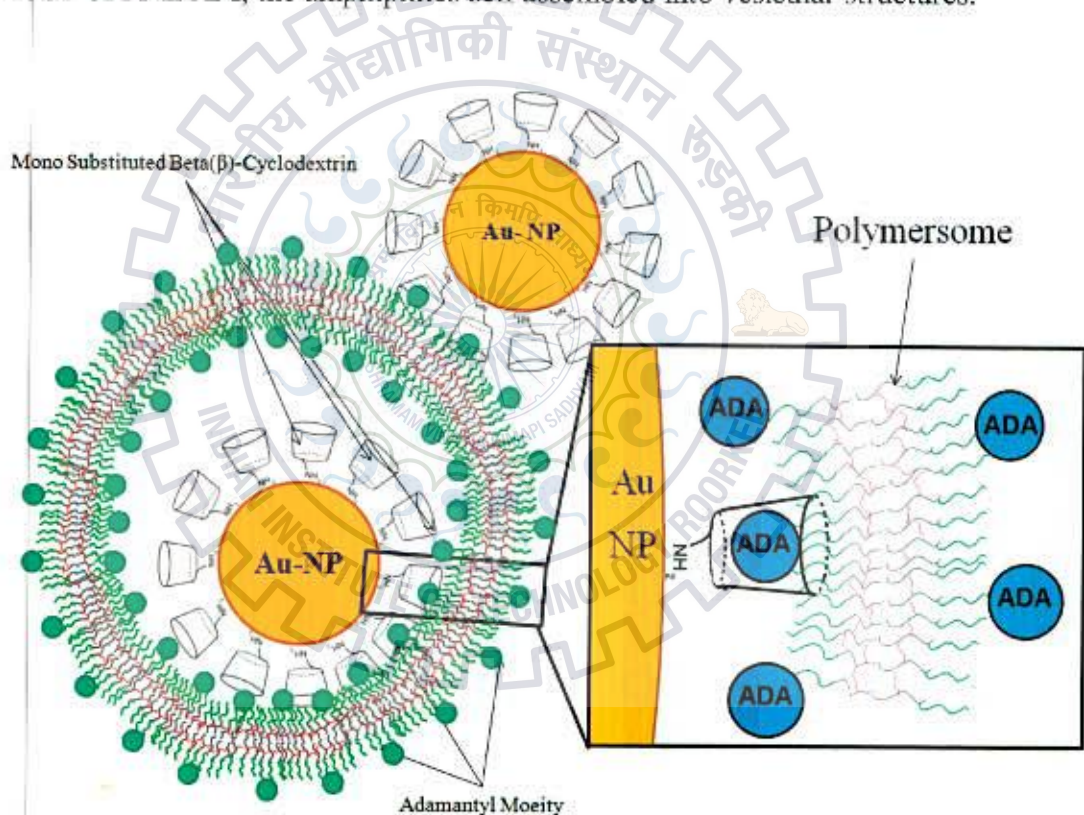


Figure 9: AuNP uptake by polymersome due to β -cyclodextrin-Adamantane host guest interaction

To incorporate this host-complexation process into our AuNP-polymersome system, we will adopt a different approach. It is well known that thiols and amines form self assembled monolayers on a gold surface. The amphiphiles are adsorbed on the metal surface by chemisorption through a terminal functional group to create a stable interface (73). Our concept is to modify the gold nanoparticles by amino-substituted β -Cyclodextrin by covalent chemisorption of the amine functional group on the gold surface. Adamantyl moiety will be present as an end group in the hydrophilic PEG

unit of the block copolymer used for polymersome formation. On self-assembly, the adamantyl moiety will statistically locate itself on the interior as well as exterior of the polymersome structure. On introducing the gold nanoparticles during self-assembly, it might be possible for the β -Cyclodextrin modified AuNPs to form inclusion complexes with the Adamantyl moiety on both sides of the membrane structure.



3 Experimental Section

3.1 Polymersome preparation

pH sensitive block copolymer poly-(ethyleneglycol)-block-poly-[2-diethylamino ethylmethacrylate-stat-benzophenone] [PEG₄₅-b-P(DEAEMA_x-stat-BMA_y)] was obtained from a co-worker and used for preparation of pH responsive polymersomes. The polymersome preparation protocol described by Yassin et.al, was adopted (74). To briefly describe, the block copolymer solution with concentration of 1 mg/mL was prepared by dissolving it in an acidic solution of pH 2 along with constant stirring. For initial investigations, two different acid mediums, one citric acid and the other hydrochloric acid solution whose pH were adjusted to 2 were used for block copolymer dissolution. The basic motivation being that citric acid is a weak acid and would therefore not interact strongly with the gold nanoparticles which would be used in subsequent encapsulation methods. After complete dissolution of the block copolymer, the solution was filtered with an 0.2 µm Nylon filter to remove any impurities which might disturb the self assembly process. Thereafter, the pH of the solution was gradually increased to 10 with drop-wise addition of 1M NaOH solution.

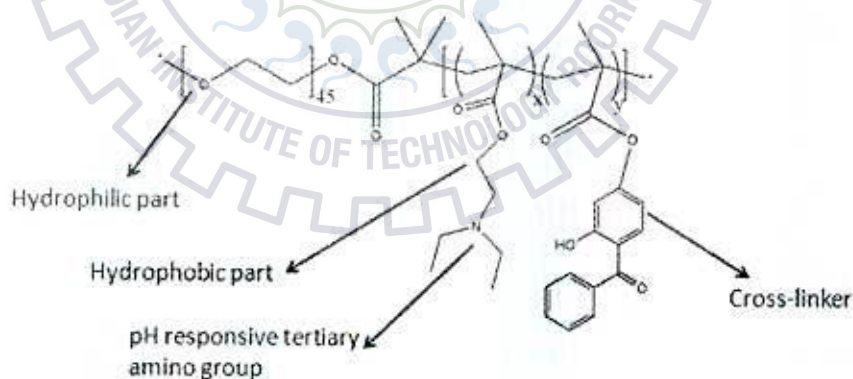


Figure 10: Chemical Structure of pH sensitive block copolymer poly-(ethyleneglycol)-block-poly-[2-diethylamino ethylmethacrylate-stat-benzophenone] [PEG₄₅-b-P(DEAEMA_x-stat-BMA_y)]

The polymersome solutions were then stirred at 430 rpm at room temperature for a minimum of three days to allow sufficient time for self-assembly process. To create shape-persistent and stable polymersomes, the samples were then crosslinked for 30 minutes under UV irradiation. Prior to cross-linking, the polymersome samples were filtered with an 0.8 µm Nylon filter to remove large aggregates if any. The irradiation

process was performed using UVACUBE100 (Honle UV Technologies, Germany) equipped with a low intensity (0.1 W/cm^2) iron lamp as UV source.

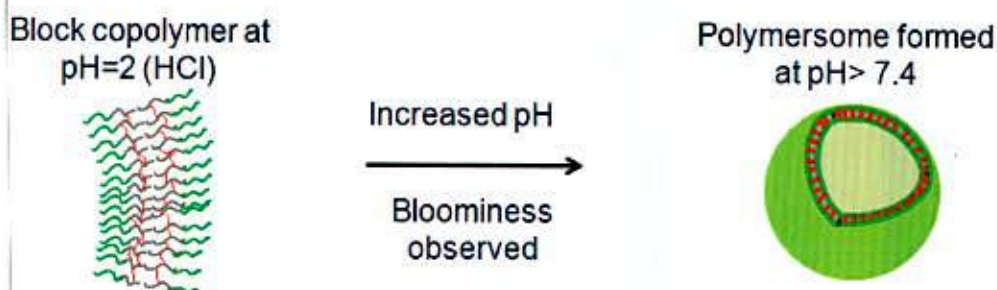


Figure 11: Schematic diagram showing pH-responsive polymersome formation

Table 3: Sample information for polymersome preparation

Sample Id	Conc. of block copolymer used (mg/mL)	Acid used for dissolution	Observation	Polymersome formation
S01	0.5	Citric acid	Bloominess observed	Yes
S02	1	Citric acid	No bloominess observed	No
S03	0.5	Hydrochloric acid	Bloominess observed	Yes
S04	1	Hydrochloric acid	Bloominess observed	Yes

The size dimensions and the polydispersity index of the prepared samples were measured by dynamic light scattering (DLS). For further preparation of polymersomes acidic solution of hydrochloric acid was used for reasons discussed in section 4.1.

3.2 Direct encapsulation of gold nanoparticles in polymersomes

3.2.1 Preliminary trial encapsulation for 12 nm gold nanoparticles

After the initial polymersome formation protocol with citric acid was discarded as unsuitable, hydrochloric acid was consistently used for polymersome formation as described by Yassin et.al (74). As method previously, the encapsulation of gold nanoparticles was to be carried out during the self-assembly process of the polymersomes. Since, a pH sensitive environment was utilised for preparation of

polymersomes, it was also imperative to determine a suitable pH in which the gold nanoparticles would be introduced into the system, since they have a tendency to agglomerate in strongly acidic or basic solutions. For the preliminary encapsulation trials, gold nanoparticles of diameter 12 nm were used. The gold nanoparticles which were obtained from Particular GmbH, had no additional capping agents to improve their stability. The concentration of this gold nanoparticle stock solution was 10 mg/L. Therefore, the block copolymer with an initial concentration of 1 mg/mL was dissolved in acidic solution (HCl) at pH 2. After complete dissolution, the pH of the solution was increased to 5 and the 12 nm gold nanoparticles were added drop-wise along with constant stirring. To initiate self-assembly of the polymersomes, the pH of the solution was slowly increased to 10 followed by stirring for three days and then cross-linking for 30 minutes. Since, the final concentration of the block copolymers in the solution was different following the addition of the gold nanoparticles, blank polymersomes with the same block copolymer concentrations were prepared for comparison. The hydrodynamic diameter and the polydispersity index of the samples were measured by dynamic light scattering (DLS).

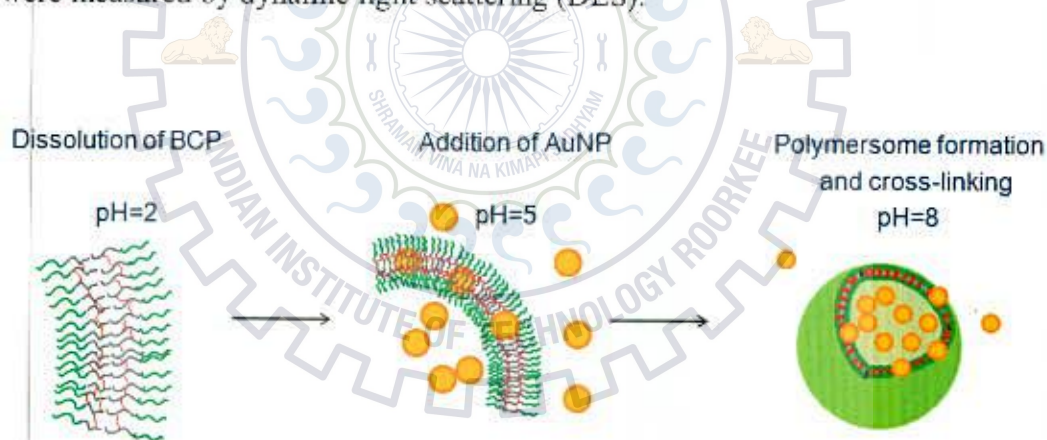


Figure 12: Schematic diagram showing direct encapsulation of 12 nm AuNP in polymersomes

Table 4: Sample information for encapsulation of 12 nm AuNP in polymersome

Sample Id	SP01	SP02
Initial BCP conc. (mg/mL)	1	1
Final BCP conc. (mg/mL)	0.5	0.7
AuNP: BCP molar ratio	1:1	0.5:1

The non-encapsulated gold nanoparticles were separated from the solution by performing Hollow Fibre Filtration (HFF). The membrane used for filtration had a

molecular weight cut-off (MWCO) of 500 kDa. A control experiment was performed to ensure that the membrane specifications were adequate to remove the 12 nm gold nanoparticles. A trans-membrane pressure (TMP) of 150 mbar was maintained during the filtration process in order to ensure that the polymersomes were not damaged. UV-vis spectra analysis was performed for the blank polymersomes (which had no additional gold nanoparticles), the 12 nm gold particle encapsulated polymersomes and the sample after filtration by HFF. The results are discussed in section 4.2.

3.2.2 Encapsulation of 30 nm citrate stabilised gold nanoparticles

The preliminary trials with 12 nm gold nanoparticles provided important insights which were used during the encapsulation experiments for the larger gold nanoparticles. As discussed in section 4.2.1, the DLS results for the 12 nm AuNP encapsulated polymersomes were not very conclusive owing to the different final concentrations of the block copolymer in the samples. Therefore, for subsequent encapsulation experiments, the initial concentration of the block copolymer was so adjusted that after the addition of the gold nanoparticles to the system, a final block copolymer concentration of 1mg/mL was achieved.

The gold nanoparticles used for encapsulation were 30 nm in diameter, with a concentration of 53.1 mg/L and were obtained by Strem Chemicals Inc. Although the gold nanoparticles were stabilised by citrate ligands (surfactant conc. = 0.1mM) which provide some stability by electrostatic interactions, even they are unstable under strongly acidic or basic conditions. Therefore, for the encapsulation in polymersomes, the same protocol of direct incorporation as was followed for the 12 nm AuNP, was adopted. After the initial block copolymer dissolution and pH increase to 5, the gold nanoparticles were incorporated to the block copolymer solution. Polymersome formation was facilitated by increasing pH to 10 followed by stirring for a minimum of 3 days and cross-linking of the samples for 30 minutes under UV-irradiation. Blank polymersome with a final block copolymer concentration of 1mg/mL was also prepared in the same conditions for comparison. As seen in the UV-vis analysis for 12 nm encapsulated polymersomes, the absorbance maxima peak for the samples was too low owing to the low concentration of the stock gold nanoparticles solution. Therefore, two samples with AuNP:BCP molar ratio of 1:1 and 5:1 were prepared for investigation.

The hydrodynamic diameter and the polydispersity index of the samples were measured by dynamic light scattering (DLS). However, separation of the 30 nm non-encapsulated AuNPs from the polymersome sample was not possible. This was because when a control experiment with the gold stock solution was performed using a membrane with MWCO of 500 kDa, the pore size was too small for the filtration. Moreover, due to unavailability of membranes with higher MWCO, HFF filtration could not be performed for the 30 nm AuNP encapsulated polymersomes. UV-vis spectra analysis of these samples would therefore have been insufficient to conclusively prove the encapsulation of the gold nanoparticles within the polymersomes. Hence, for concrete evidence of AuNP incorporation, the samples were analysed by Cryo-TEM. The results of the samples obtained by these characterisation techniques are discussed in detail in section 4.2.2.

3.2.3 Encapsulation of 60 nm citrate stabilised gold nanoparticles

Gold nanoparticles with a mean hydrodynamic diameter of 60 nm, and a concentration of 100 mg/L, were obtained by Strem Chemicals Inc. The gold nanoparticles were also stabilised by citrate ligands with a concentration of less than 0.01 mM. Two different samples with AuNP:BCP molar ratio of 1:1 and 5:1 were prepared using the same protocol as employed for the 30 nm AuNP. After the preparation of the samples, DLS analysis was carried out to determine their hydrodynamic diameter and the polydispersity index. However, as in the case of 30 nm AuNP, Hollow Fibre Filtration to separate the non-encapsulated gold nanoparticles could not be performed. Therefore, once again Cryo-TEM investigation of the samples was done to ascertain the encapsulation efficiency in the polymersomes. Detailed discussion of the experimental results can be obtained in section 4.2.2.

3.3 PEG-AuNP hybrid interactions

As discussed in section 2.3.3, there are numerous challenges in attempting to incorporate such large gold nanoparticles (30 nm and 60 nm) in polymersomes. Therefore the first strategy adopted to selectively guide the gold nanoparticles towards the polymersomes was the use of PEG-PEG interactions as discussed in section 2.4.1 to result in the formation of a possible PEG-AuNP hybrid system. Surface

modification studies of the gold nanoparticles were performed with two ligands, MeO-(PEG)₇-SH [M.W. = 356.48 g/mol] and MeO-(PEG)_n-SH [M.W. = 2000 g/mol].

Prior to carrying out the modifications, it was essential to determine the ligand concentration required to saturate the available gold surface. For this purpose, the estimated binding surface area of MeO-(PEG)₇-SH gathered from literature was found to be 20 Å² and that for the ligand MeO-(PEG)_n-SH was 40 Å². Theoretical calculations were performed to calculate the ligand concentrations. Using these values, a series of titration plans for surface modification were generated using the in-house UV-vis Tools software. Since the saturation ligand concentrations were only theoretical values, modification experiments were also carried out at ligand concentrations below and above the calculated values to ascertain their practicality.

For the modification experiments, 1 mL of the gold nanoparticles solution was placed in a 1.5 mL quartz cuvette and was sealed with a septum. According to the titration plans, measured volumes of the ligand solution were injected into the cuvette with a microlitre syringe. After every titration step, the system was homogenized and kept for 5 minutes to attain equilibrium. UV-vis spectra was measured in the wavelength range of 400-650 nm for every titration to monitor the surface modification process, since addition of ligand solution would affect the surface plasmon resonance band of the gold nanoparticles. The individual spectra for each of the titration steps were plotted and the wavelength corresponding to their absorbance maxima were determined. Plotting these values against their respective ligand concentrations provided a clear idea about the extent of surface modification of the gold nanoparticles.

The PEGylated gold nanoparticles were also analysed by DLS and TEM to select the most preferable ligand for this PEG-AuNP hybrid experiment. As discussed in section 4.3, the MeO-(PEG)_n-SH [M.W. = 2000 g/mol] was found suitable for surface modification of the gold nanoparticles. Final ligand concentration of 4.2×10⁻³ M was employed for preparation of modified AuNPs and their subsequent incorporation in polymersomes. Two different samples SP 63 and SP76 were prepared with all the same conditions, except the mode of addition of the PEGylated gold nanoparticles.

Table 5: Sample Information for PEG-AuNP hybrid

Sample Id	SP63	SP76
Wt. % of unfunctional BCP	100	100
Final BCP conc. (mg/ml)	1	1
AuNP : BCP ratio	4:1	4:1
Ligand concentration (M)	4.2×10^{-3}	4.2×10^{-3}
Method of AuNP addition	During self-assembly	Preformed polymersomes

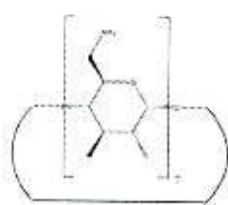
DLS measurements were performed for both the samples to determine the hydrodynamic diameter and polydispersity index. UV-vis analysis was performed to check for possible shift in plasmon resonance band due to the formation of a potential AuNP-PEG hybrid structure. Gold nanoparticle incorporation in polymersomes was investigated by Cryo-TEM for sample SP63, but not for sample SP76 due to insufficient time.

3.4 Threading interaction between PEG and β -cyclodextrin

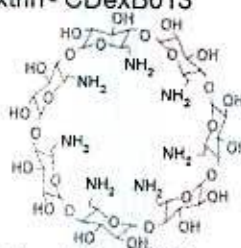
The formation of inclusion complex by threading interaction between PEG chains and β -cyclodextrin cavity has already been discussed in section 2.4.2. The first step in this approach was the surface modification of the gold nanoparticles with amine functionalised β -Cyclodextrin. It is well known that an amine group has comparatively lesser affinity for gold than thiol ligand. Therefore, two different amine-functionalised β -Cyclodextrins were used for AuNP surface modification.

- Heptakis-(6-amino-6-deoxy)- β -cyclodextrin [CDexB053] – fully substituted β -Cyclodextrin
- 6-Monodeoxy-6-monoamino- β -cyclodextrin [CDexB013] – mono substituted β -Cyclodextrin.

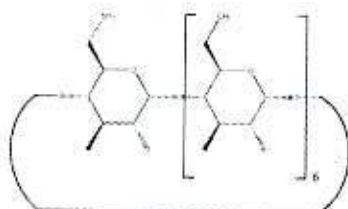
Heptakis-(6-amino-6-deoxy)- β -cyclodextrin - CDexB013



=



6-Monodeoxy-6-monoamino- β -cyclodextrin - CDexB053



=

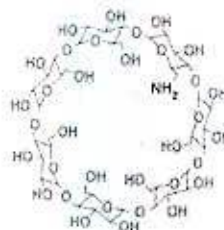


Figure 13: Aminated β -Cyclodextrin Ligands used for Au-NP surface modification

Both the β -Cyclodextrin ligands were obtained from AraChem Cyclodextrin Shop. The estimated binding surface area of CDexB013 gathered from literature was found to be 40 \AA^2 and that for the ligand CDexB053 was 400 \AA^2 and theoretical calculations were performed to determine the saturation ligand concentrations. As described in section 4.3, titration plans were created for each of the ligands and UV-spectra was analysed after each titration step.

For the modification experiments, 1 mL of the gold nanoparticles solution was placed in a 1.5 mL quartz cuvette and was sealed with a septum. Since, the β -Cyclodextrin ligands were supplied in the form of chloride salts it was necessary to deprotonate them and thus activate the amine functional groups before carrying out the surface modification of the gold nanoparticles. Therefore, the ligand solids were dissolved in phosphate buffer saline (PBS) solution of pH 8 and 10 mM strength for a minimum of 2 hours to allow for complete deprotonation of the β -Cyclodextrin. Titration experiments were performed as described in the previous section. After every titration step, the system was homogenized and kept for 5 minutes to attain equilibrium. UV-vis spectrum was measured in the wavelength range of 400-650 nm for every titration to monitor the surface modification process. The wavelength corresponding to absorbance maxima were then plotted against their respective ligand concentrations to get a clear idea about the extent of surface modification of the gold nanoparticles.

The citrate stabilized 60 nm gold nanoparticles were surface modified with both the ligands, CDexB013 and CDexB053. The hydrodynamic diameter and polydispersity index of the samples were measured in comparison to the unmodified blank AuNPs after overnight equilibration. As discussed in section 4.4.1, the gold nanoparticles modified with CDexB013 were deemed unsuitable for use in encapsulation experiments. Therefore, for the incorporation of gold nanoparticles in polymersomes, the heptakis-(6-amino-6-deoxy)- β -cyclodextrin [CDexB053] – mono amino substituted β -Cyclodextrin was used.

For polymersome formation, the un-functional block copolymer [PEG₄₅-b-P(DEAEMA_x-stat-BMA_y)] was used. The motivation behind this concept was that the PEG chains comprising the block copolymer would fit inside the β -Cyclodextrin cavity to form inclusion complex and the gold nanoparticles attached to the β -Cyclodextrin moiety would be incorporated in the polymersome. Again a two-pronged method was adopted to study this possible interaction. β -Cyclodextrin modified gold nanoparticles were added both during self-assembly process of the polymersomes and also to pre-formed polymersomes.

Table 6: Sample Information for threading interaction

Sample Id	SP62	SP75
Wt. % of unfunctional BCP	100	100
Final BCP conc. (mg/ml)	1	1
AuNP : BCP ratio	4:1	4:1
Method of AuNP addition	During self-assembly	Preformed polymersomes

DLS measurements were performed for both the samples to determine the hydrodynamic diameter and polydispersity index. UV-vis analysis was performed to check for possible shift in plasmon resonance band owing to inclusion complexation. Gold nanoparticles incorporation was investigated by Cryo-TEM for sample SP62.

3.5 Gold nanoparticle uptake in polymersomes using host-guest complexation

Host-guest complexation of Adamantane with β -Cyclodextrin to selectively guide the gold nanoparticles incorporation in polymersomes was explained in section 2.4.1. The first step for the AuNP uptake by host-guest complexation strategy was similar to the threading interaction. The 60 nm AuNPs were modified with the CdexB053 ligand. For the polymersome formation a mixture of the un-functional block copolymer [PEG₄₅-b-P(DEAEMA_x-stat-BMA_y)] and the same block copolymer with Adamantane end groups(Ada-BCP) was used. In our system, during polymersome formation, the block copolymers would self-assemble statistically where-in some of the Adamantane groups would be on the periphery of the polymersome and some on the inside. The mono-amino substituted β -cyclodextrin is used for modification of the gold nanoparticles. However if complete surface modification is carried out then the β -cyclodextrin: Adamantane molar ratio would shoot up to 10:1 if a mixture containing 80 wt. % unfunctional BCP and 20 wt% Ada-BCP is used. Since the concentration of the gold nanoparticles stock solution is fixed, the only option is to go for partial modification of the gold nanoparticles surface resulting in a lower ligand concentration. Therefore, finally the β -cyclodextrin ligand concentration is fixed at $6.5 \times 10^{-5} \text{M}$ leading to a β -cyclodextrin: Adamantane molar ratio of 3:1.

Although it was discussed in section 4.2.2, that incorporation of gold nanoparticles might affect self-assembly process, one trial experiment was performed where the β -cyclodextrin modified AuNPs were added during self-assembly process. For subsequent experiments using host-guest chemistry, three different samples with β -cyclodextrin: Adamantane molar ratio of 1:1, 2:1 and 3:1 were prepared to study the effect of host-guest complexation on gold nanoparticles uptake in polymersomes. In these experiments, the β -cyclodextrin modified gold nanoparticles were added to preformed polymersomes comprising 80 wt. % unfunctional BCP and 20 wt% Ada-BCP. The samples were stirred for a period of 20 hours at 430 rpm to allow sufficient time for the system to attain equilibrium and the formation of the host-guest complex.

Table 7: Sample information for host-guest complexation

Sample Id	SP61	SP72	SP73	SP74
Wt. % of unfunctional BCP	80	80	80	80
Wt % of Adamantane - BCP	20	20	20	20
Final BCP conc. (mg/ml)	1	1	1	1
β -cyclodextrin : Adamantane ratio	3:1	1:1	2:1	3:1
Method of AuNP addition	During self-assembly	Preformed polymersomes	Preformed polymersomes	Preformed polymersomes

The samples were analysed by DLS for measuring the hydrodynamic diameter and polydispersity index. UV-vis spectra of the samples were measured to investigate possible change in plasmon resonance of the gold nanoparticles due to the host-guest complexation. Finally, Cryo-TEM analysis was performed for the sample SP61 to investigate the gold nanoparticles incorporation in the polymersomes. However due to insufficient time, Cryo-TEM analysis of the samples SP72, SP73 and SP74 could not be performed.

3.6 Characterisation techniques and instrumentation

3.6.1 Dynamic light scattering

The dynamic light scattering measurements of the all the samples were performed by using the Zetasizer Nanoseries instrument (Malvern, UK) fitted with a Helium-Neon laser (4 mW, $\lambda = 632.8$ nm). All measurements were performed at 25°C using disposable plastic cuvettes. The data was collected by non-invasive back scattering method at a fixed angle of 173°.

For the polymersome samples along with the gold nanoparticle incorporated polymersomes, the material used in the standard operating procedure (SOP) was set for polyethyleneglycol (PEG) so that its refractive index and absorption co-efficient

were used in the calculations. But for DLS measurement of the blank gold nanoparticles as well surface modified gold nanoparticles, the material specified in the SOP was gold. However, since all the systems were in aqueous phase, water was indicated as the dispersant indicated in the SOP. An equilibration time of 120 seconds was allowed for each sample with three measurement trials consisting of ten runs each. All the peak sizes calculated were z-averaged over all the measurement values.

3.6.2 UV-vis spectroscopy

For the UV-vis spectroscopy measurements, a two-beam spectrometer Lambda 800 (PerkinElmer, USA) spectrometer was used. For the polymersome samples, a spectral wavelength range from 900-200 nm was used. In case of the gold nanoparticles as well as the ligand modified gold nanoparticles, measurements were performed in the range of 650-400 nm. A scanning speed of 375 nm/min with an integration time of 0.012 seconds was used for all the measurements. For all the measurements, 10 mm quartz cuvettes were used.

3.6.3 TEM measurements

For the TEM measurements of the gold nanoparticles as well as Cryo-TEM measurements of the polymersome samples, Libra 120 microscope (Zeiss, Germany) with an operating acceleration voltage of 120 keV was used. Samples were mounted on copper Quantifoil Grids with 1.3 micrometers holes. 3.5 μ l of the solution were placed on the grid and blotted from the back side for 3.2 seconds at relative humidity 88%. For the Cry-TEM analysis, an additional step involving flash-freezing in liquid ethane at a temperature of -178°C was performed. All images were taken in Bright Field at -172° .

3.6.4 UV irradiation

Cross-linking of the polymersome samples by exposure to UV irradiation was performed using UVACUBE (honle UV Technologies). A low intensity (0.1 W/cm^2) iron lamp served as the UV source.

3.6.5 Hollow fibre filtration

The hollow fibre filtration (HFF) of the 12 nm encapsulated polymersomes was performed using a KrosFlo Research Ili (SpectrumLabs, USA). A polysulfone-based separation module (MWCO: 500 kDa, Spectrum Labs, USA)) was employed as the separation membrane along with a trans-membrane pressure (TMP) of 150 mbar.



4 Results and discussions

4.1 Polymersome formation

4.1.1 Dynamic light scattering results

The samples S01, S03 and S04 were analysed by Dynamic light scattering with the appropriate measurement parameters as described in section 3.6.1. Fig. 14 shows the intensity plot against the hydrodynamic diameter of sample S04, which has a BCP conc. of 1 mg/mL prepared in HCl solution. The curves of the three measurement trials are well overlapped and with sharp narrow peaks, which indicates that the polymersomes formed have a homogeneous size distribution. The low Polydispersity index value (PDI) also corroborates this observation.

Table 8: DLS investigation results of pH responsive Polymersomes formed.

Sample Id	Conc. of block copolymer used (mg/mL)	Acid used for dissolution	Z _{avg} Diameter of polymersome (nm)	Polydispersity index (PDI)
S01	0.5	Citric acid	168.4	0.17
S03	0.5	Hydrochloric acid	109.1	0.16
S04	1	Hydrochloric acid	152.7	0.17

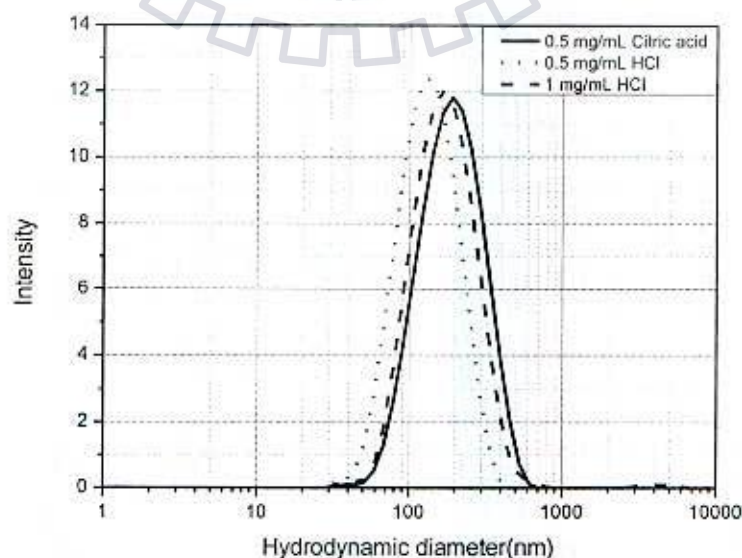


Figure 14: Intensity averaged diameter plot for polymersomes formed in various acid environments obtained using DLS

A polydispersity index value around 0.15 generally indicates a sample with a narrow size distribution as in the case of these polymersomes. It was already clear from the absence of bloominess in case of sample S02 that polymersome formation did not occur. This same experiment was repeated twice, but with no positive results. Therefore it was apparent that, the polymersome formation was not suitable in case of citric acid being used as the acid. The dissolution of the block copolymers in citric acid took much longer than in hydrochloric acid, because citric acid is a weaker acid in comparison. During polymersome formation also, it was observed that citric acid due to its buffer like behaviour hinders the smooth increasing of pH. It also results in dilution of the polymersome solution because large volume of the base (NaOH) is required to change the pH of the system. Moreover, a sudden pH transition is observed at 6.8 in case of citric acid leading to possible experimental errors in polymersome formation. Therefore, the previously well established protocol of using hydrochloric acid solution for preparation of further polymersome samples was adopted. Subsequent preparation of polymersomes with 1mg/mL concentration yielded polymersomes with sizes ranging from 110-140 nm. And for a BCP conc. of 0.5 mg/mL the sizes were in the range of 75-90nm. Since, these polymersome samples were the first trials, therefore their comparatively larger sizes might attributed to experimental errors.

4.2 Direct encapsulation of gold nanoparticles in Polymersomes

4.2.1 Encapsulation for 12 nm gold nanoparticles

4.2.1.1 Dynamic light scattering results

The gold nanoparticles encapsulated polymersome samples along with the similarly concentrated blank polymersome samples were investigated by DLS using the same set of parameters as before.

Table 9: DLS results of encapsulation for 12 nm Au NP

Sample Id	Conc. of block copolymer used (mg/mL)	AuNP:BCP molar ratio	Zavg. Diameter of polymersome (nm)	Polydispersity index (PDI)
SP01	0.5	1:1	88.4	0.22
SP01B	0.5	NA	77.9	0.16
SP02	0.7	0.5:1	92.2	0.20
SP02B	0.7	NA	90.4	0.15

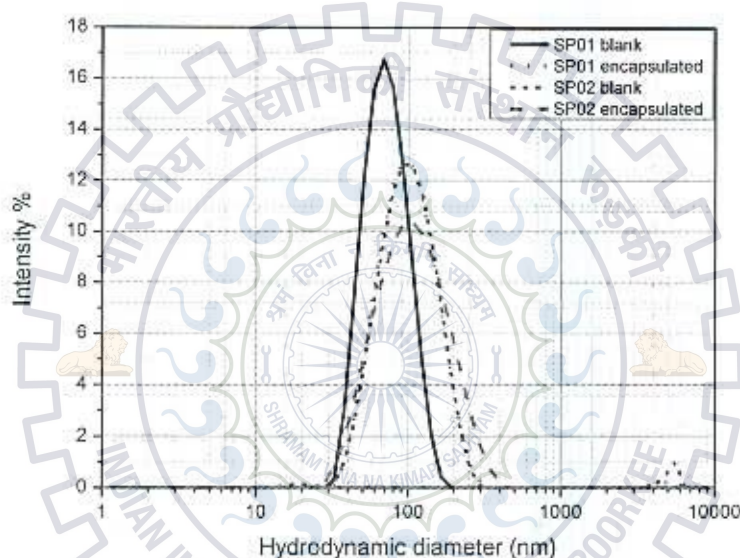


Figure 15: Intensity averaged diameter plot for 12 nm AuNP encapsulated polymersome & blank polymersome obtained using DLS

Thus, it was observed that the hydrodynamic diameter of the polymersome encapsulated with AuNP is larger than that of the blank polymersome. This increase in size is more substantial in case of sample SP01 than in case of sample SP02. This might be due to the fact that SP01 has larger amount of gold nanoparticles incorporated in the system which also improves the encapsulation efficiency. However, the size difference between SP02 and its blank sample is barely noticeable. Therefore, it cannot be conclusively said from the DLS results that the gold nanoparticle is encapsulated in this case. However, the polydispersity index of both the encapsulated polymersome samples is higher than the blank polymersomes larger. This might be either due to the fact that the encapsulation is successful thereby increasing the PDI or it might also be because of the fact that a completely different

system that is the gold nanoparticles, with a separate size dimension, is added to the previously comparatively mono-disperse polymersome sample. Additionally, it was also observed that as the block copolymer concentration increases the size of the polymersome also increases.

To summarise, investigation by Dynamic Light Scattering could not provide solid evidence of gold nanoparticle encapsulation within the polymersome. Moreover, the different final concentration of the block copolymer in the samples after gold nanoparticle addition makes it difficult to derive worthwhile conclusions from the DLS investigations. Keeping this in mind, for further encapsulation experiments involving the larger gold nanoparticles, the final block copolymer concentration in the system was always maintained at 1mg/mL.

Therefore, the samples were filtered by HFF as described in section 4.2 and UV-vis investigations were performed for conclusive evidence of gold nanoparticle encapsulation.

4.2.1.2 UV-vis spectroscopy results

As previously stated, Hollow fibre filtration was performed to separate the non-encapsulated gold nanoparticles from the encapsulated polymersome samples. UV-vis spectra was measured in the range of 200-900 nm for the blank polymersome sample, the gold nanoparticles encapsulated polymersome prior to HFF and lastly, of the gold nanoparticle encapsulated polymersome after purification by HFF.

As can be seen from graph in fig. 16, the 12 nm gold nanoparticles exhibit their characteristic surface plasmon resonance at a wavelength (λ_{max}) of 519 nm corresponding to maximum absorbance. The sample SP01 shows this same peak at 519 nm in case of both, before HFF which is obvious, but even after purification by HFF. This clearly shows the presence of gold nanoparticles even after filtration. To discount the possibility that there might be stray gold nanoparticles present after HFF, a control experiment was performed with just the gold nanoparticle stock solution purification by HFF. The residual solution after purification was then measured with UV-vis to check for the peak due to presence of traces of gold nanoparticles. However, no such peak was observed. Therefore it would be logical to say that the peak observed after HFF of the encapsulated polymersome sample, is due to the gold

nanoparticles that are present within the polymersome. Additionally, there is a decrease in absorbance at λ_{\max} after HFF which also conclusively proves the removal of the non-encapsulated gold nanoparticles. However, the peak observed at 519 nm after purification is a distinct but mild peak indicating that few number of gold nanoparticles are encapsulated within the polymersome.

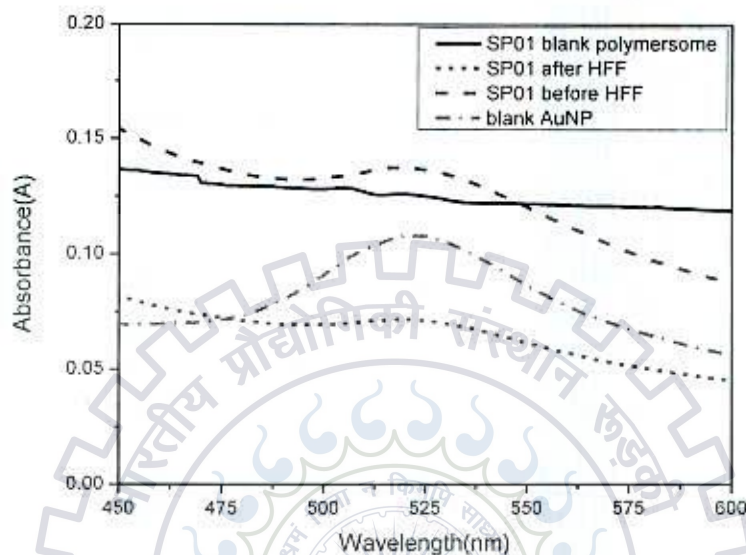


Figure 16: Absorbance vs. Wavelength for SP01 blank polymersome, SP01 after HFF, SP01 before HFF and blank AuNP obtained using UV-vis spectroscopy

Upon performing HFF of the sample SP02 and its subsequent analysis by UV-vis spectra, barely any peak at 519 nm could be observed. This might be due to the fact that there was lesser amount of gold nanoparticles present at the start than in case of SP01. Therefore, even though there might be some gold nanoparticles which are encapsulated within the polymersomes, their number is so few that they do not show a distinct peak at 519 nm. Hence, for later encapsulation experiments with the 30 nm and 60 nm gold nanoparticles, larger AuNP:BCP molar ratios were used.

4.2.2 Encapsulation for 30 nm gold nanoparticles

4.2.2.1 Dynamic light scattering results

The gold nanoparticle encapsulated samples as well as the blank polymersome sample prepared in the same conditions were analysed using DLS with the same parameters as before.

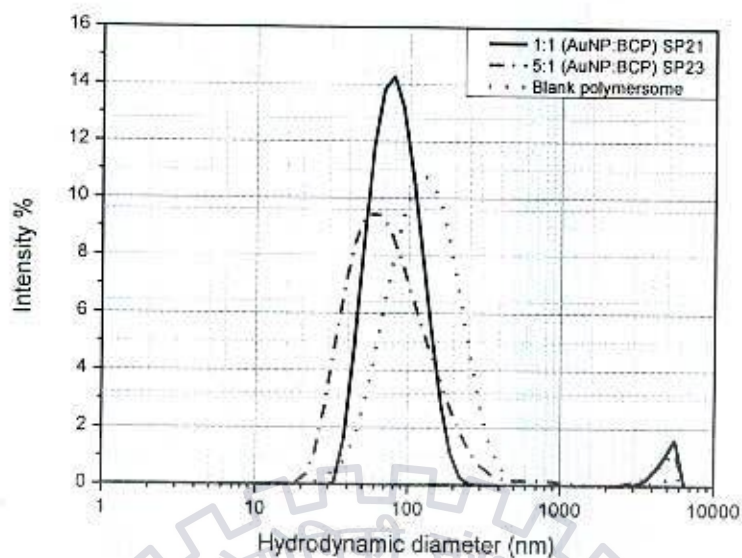


Figure 17: Intensity averaged diameter plot for 30 nm AuNP encapsulated polymersome obtained using DLS

Table 10: DLS analysis of 30 nm AuNP encapsulated

Sample Id	Final conc. of BCP(mg/mL)	AuNP : BCP molar ratio	Zavg. Diameter of polymersome (nm)	Polydispersity index (PDI)
SP21	1	1:1	85.8	0.24
SP23	1	5:1	73.8	0.33
Blank polymersome	1	NA	115.7	0.16

Surprisingly, the DLS investigations revealed a decrease in the size of the gold nanoparticle encapsulated polymersomes in comparison to the size of the blank polymersome. Sample SP23 which had a higher gold nanoparticle molar ratio showed a larger size reduction than sample SP21 with equimolar gold nanoparticle concentration. However, the polydispersity index of the encapsulated samples was higher than the blank polymersome similar to the trend observed for the 12 nm gold nanoparticle encapsulated polymersomes. A possible explanation for the size reduction, might be that addition of gold nanoparticles to the polymersome system causes possible disruptions in the polymersome self-assembly process. Although, it might also be argued that why such a trend is not observed in case of the 12 nm gold nanoparticles. But before making this statement we must bear in mind that size ratios

of the gold nanoparticles and polymersomes are an important factor while considering encapsulation processes. Therefore, it may be postulated that the large size of the gold nanoparticles as in case of the 30 nm AuNP might be more detrimental to self-assembly of polymersomes than the smaller sized 12 nm AuNP.

As already mentioned in section 4.2, due to unavailability of membranes with higher MWCO, HFF filtration could not be performed for the 30 nm AuNP encapsulated polymersomes. Therefore, investigation by UV-vis would not have provided any real clue about the encapsulation efficiency of the gold nanoparticles by the polymersomes. Hence, for conclusive evidence about the extent of AuNP incorporation within the polymersomes, Cryo-TEM analysis was performed for the samples.

4.2.2.2 Cryo TEM results

The samples SP21 and SP 23 which were prepared by in-situ addition of gold nanoparticles during self-assembly were analysed by Cryo-TEM. The samples for the measurement were prepared as described in section 3.2.2.

The sample SP21 had a AuNP:BCP molar ratio of 1:1. The blue arrows in Fig 18a show the polymersomes. The bilayer membrane structure of the polymersomes is clearly visible in this image. The two dark, opaque spheres are the 30 nm gold nanoparticles. The gold nanoparticle marked by the green arrow is completely encapsulated within the internal hydrophilic cavity of the polymersome.

In fig. 18b, the encircled region marked by red arrow shows an example of a gold nanoparticle partially engulfed by the polymersome membrane. In all the images, the number of the polymersomes far exceeds the number of the gold nanoparticles on the TEM grid.

Sample SP23 has a higher AuNP:BCP molar ratio of 5:1. Fig 19a has two encircled regions which are of particular interest. The green arrows again show examples of gold nanoparticles completely internalised within the polymersome cavity. The red arrows on the other hand point to gold nanoparticles which have partial engulfment interactions with the polymersome membrane.

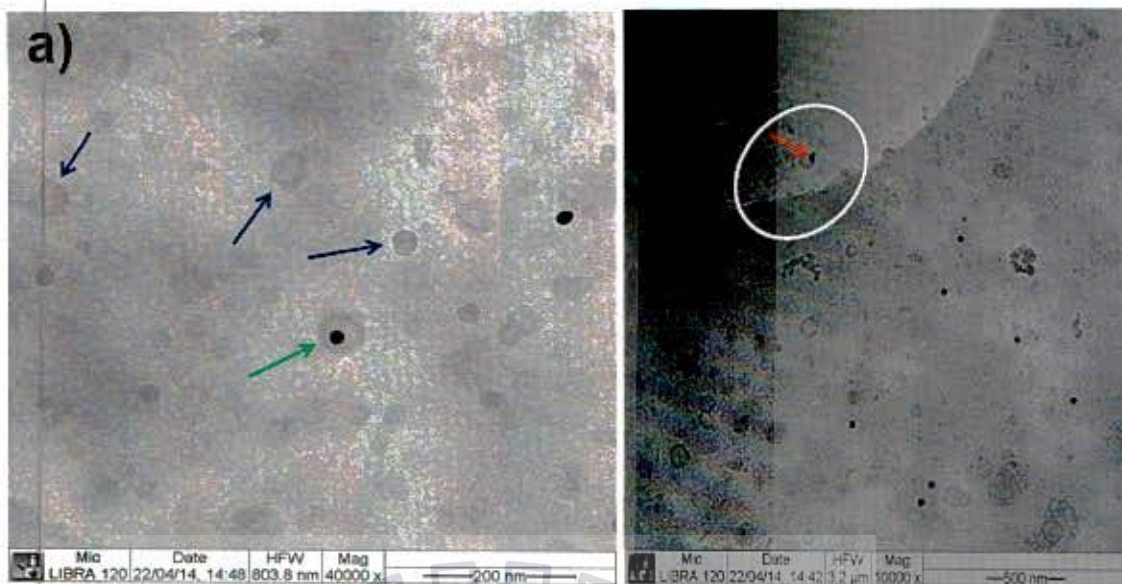


Figure 18: Cryo-TEM images of SP21- 30 nm AuNP interacting with Polymersome. a) shows Au NP engulfed in polymersome and b) shows Au NP interacting with bilayer membrane of polymersome.

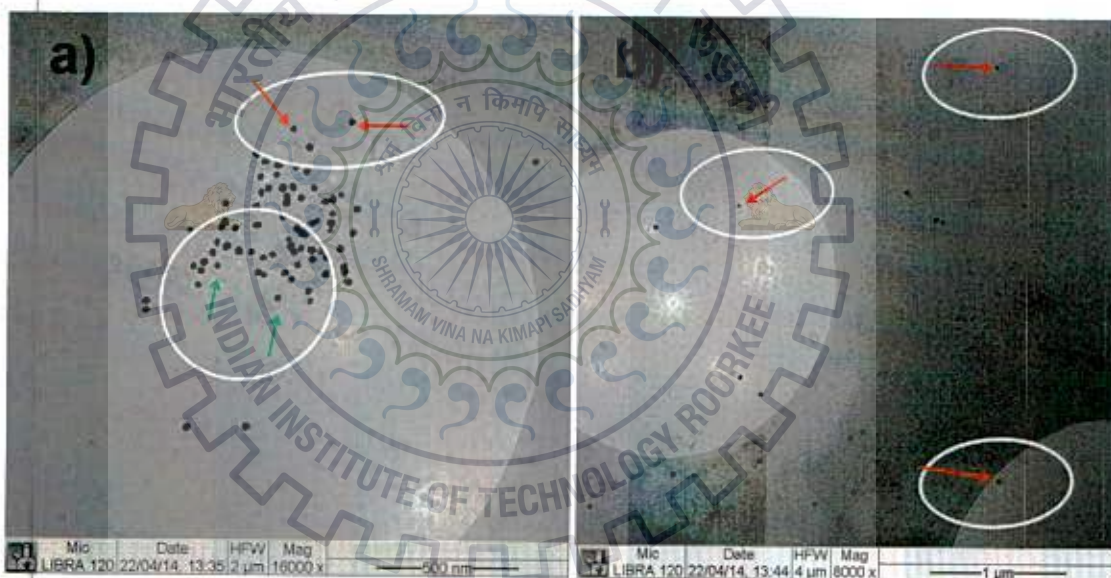


Figure 19: Cryo-TEM images of SP23- 30 nm AuNP interacting with Polymersome. a) shows Au NP engulfed in polymersome and b) shows Au NP interacting with bilayer membrane of polymersome.

Similarly in Fig 19b, the encircled regions with red arrows show more instances of partial internalisation of gold nanoparticles by the polymersome membrane. Even though there are more number of gold nanoparticles than the previous sample, there are still vast number of polymersomes. The gold nanoparticles are however well dispersed within the sample and do not show any visible aggregation tendency. Moreover, as the AuNP:BCP molar ratio increases, there is an increased chance of either complete encapsulation or partial engulfment of the gold nanoparticles with the polymersomes. However, there are still many gold nanoparticles which are randomly dispersed within the sample with little affinity for interaction with the polymersomes. All these samples were prepared by introducing the gold nanoparticles to the block

copolymer solution at pH 5. Two more samples were prepared where the gold nanoparticles were added to the block copolymer solution at pH 4, with the assumption that it might improve encapsulation efficiency of the gold nanoparticles. Further investigations however revealed that no such improvement was observed. This might be because even at pH 4, there exists some level of pre-organisation in the micellar structure which undergo re-organisation during self assembly at increased pH to form polymersomes. Due to the large size of the gold nanoparticles with respect to the polymersome membrane wall which has a thickness of about 13-18nm, encapsulation by diffusion through the membrane is not possible.

4.2.3 Encapsulation for 60 nm gold nanoparticles

4.2.3.1 Dynamic light scattering results

The hydrodynamic diameter and polydispersity index of the 60 nm gold nanoparticles encapsulated polymersome samples as well the blank polymersome sample were measured by dynamic light scattering. The parameters used during the analysis are already mentioned in section 3.6.1.

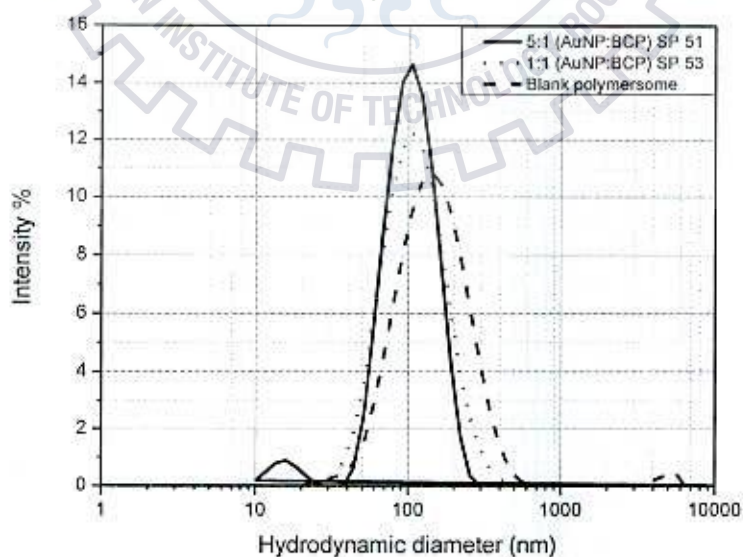


Figure 20: Intensity averaged diameter plot for 60 nm AuNP encapsulated polymersome

Table 11: DLS analysis of 60 nm AuNP encapsulated polymersomes

Sample Id	Final conc. of BCP(mg/mL)	AuNP : BCP molar ratio	Zavg. Diameter of polymersome (nm)	Polydispersity index (PDI)
SP51	1	5:1	92.7	0.24
SP53	1	1:1	101.3	0.21
Blank polymersome	1	NA	132.3	0.14

The hydrodynamic diameter and the polydispersity index for the 60 nm AuNP samples followed the same trend as shown by the 30 nm AuNP samples. The size of the encapsulated samples was smaller than that of the blank polymersome sample. The size reduction was more pronounced in case of the sample with the higher AuNP:BCP molar ratio. However, the polydispersity index for both the AuNP encapsulated samples was higher than the blank polymersome sample.

These size reduction trends again lend credence to the postulation that large size of the incorporated gold nanoparticles, might be affecting the re-organisation and self assembly process undergoing during the formation of the polymersomes. Although, no previous studies have been performed with such large sized nanoparticles, it might be said that incorporation of these large nanoparticles in polymersomes, might be causing some entropical imbalance in the system due to unfavourable size configurations.

As in the case of the 30 nm AuNP samples, these larger sized 60 nm AuNP incorporated polymersomes could also not be filtered by Hollow fibre filtration method due to unavailability of sufficiently larger pore sized membranes. Therefore, the samples were investigated by Cryo-TEM to determine if the encapsulation of the gold nanoparticles within the polymersomes was successful.

4.2.3.2 Cryo TEM results

The samples SP51 and SP 53 which were prepared by in-situ addition of gold nanoparticles at pH 5 during self-assembly were analysed by Cryo-TEM. The sample SP51 has higher AuNP:BCP molar ratio of 5:1 in contrast to the equimolar sample SP53. Fig. 21a of the sample SP51 shows a vast number of well-formed bilayered polymersomes.

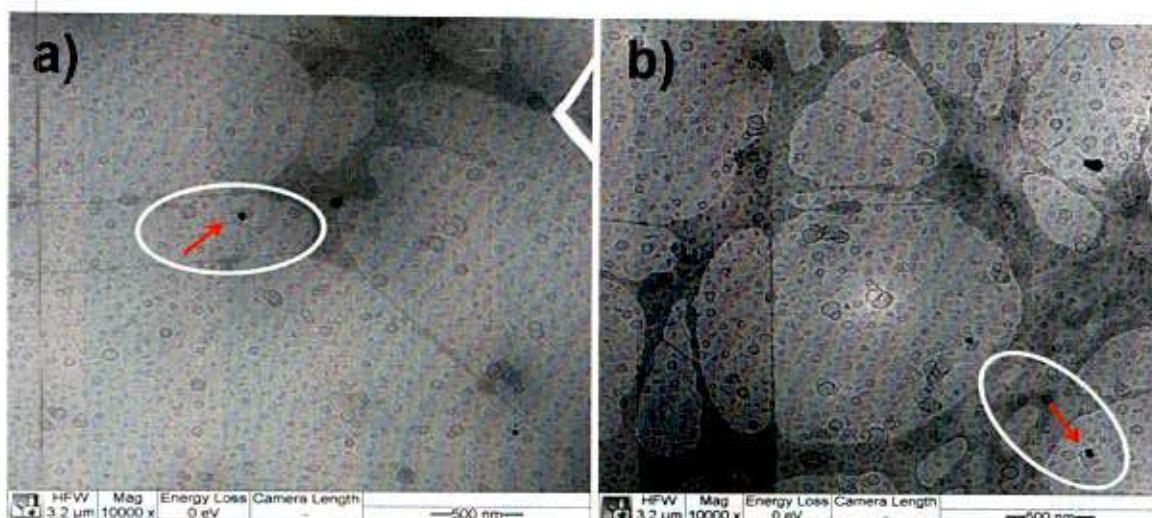


Figure 21: Cryo-TEM micrograph of sample SP51. a) shows vast number of bilayered polymersomes. b) shows partial engulfment of Au-NP in bilayered membrane of polymersome.

The encircled region marked with a red arrow shows a rare instance of partial entrapment of the 60 nm gold nanoparticle by the polymersome membrane. A similar example of partial engulfment of the gold nanoparticle can be observed in fig. 21b for the same sample.

However, no instances of complete internalisation of a gold nanoparticle within the polymersome cavity could be found. In case of sample SP53 with lower AuNP:BCP molar ratio, not a single case could be observed where the gold nanoparticle was encapsulated within the polymersome or even partially entrapped by the polymersome membrane. Therefore, in this case too we see that increasing the AuNP:BCP molar ratio increases the chance of AuNP interaction with the polymersome. It is logical because the presence of more number of gold nanoparticles itself, increases the encapsulation probability. Moreover, the complete lack of complete internalisation of the 60 nm AuNP in comparison to the 30 nm AuNP is also an important observation. This might be explained by the fact that the large size of the gold nanoparticle would create an entropically unstable system in case of its internalisation. It may also be a deterrent for partial engulfment of the nanoparticle by the membrane, because the polymer chains might be too strained by stretching to accommodate such a large particle. Therefore, it can be conclusively said that this method of direct encapsulation of gold nanoparticles by in-situ addition during self-assembly is not a very efficient process. Even though complete encapsulation within the polymersome might be difficult, partial engulfment or even gold nanoparticle interaction with the polymersome periphery might be attempted. For such endeavours, there is a need for

specific interactions to selectively guide the gold nanoparticles to the preferred location on the polymersome. The results for three such strategies mentioned in section 2.4, have been discussed in the following sections.

4.3 Gold nanoparticle uptake by PEG - AuNP hybrid

As discussed in section, the 60 nm AuNPs were modified with thiolated PEGs with different molecular weights and the effect of the ligand capping was investigated via UV-vis, DLS and TEM analysis.

4.3.1 Surface modification of 60 nm AuNP with thiolated PEGs

4.3.1.1 UV-vis spectroscopy results

Fig. 22 shows the UV spectra of the 60 nm gold nanoparticles during the surface modification experiment with the MeO-(PEG)₇-SH ligand at a calculated saturation ligand concentration of 7×10^{-3} M. A mild shift in the plasmon resonance band as well as absorbance is seen after every titration step. Fig. 23 which plots the wavelength corresponding to maximum absorbance (λ_{max}) against the solution concentration shows a plateau region indicating that the saturation of the available gold surface has been attained. A shift of 1.45 nm in plasmon resonance band of the gold nanoparticles was observed after modification.

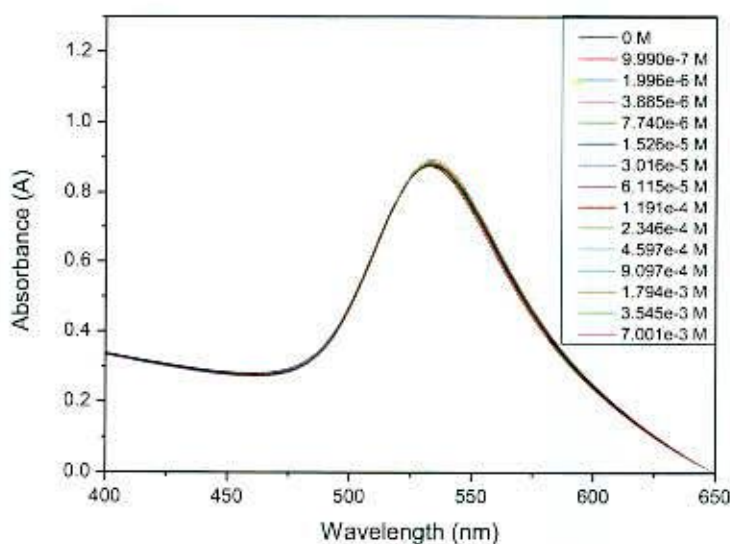


Figure 22: UV-vis spectra of 60 nm AuNP surface modification with MeO-(PEG)₇-SH

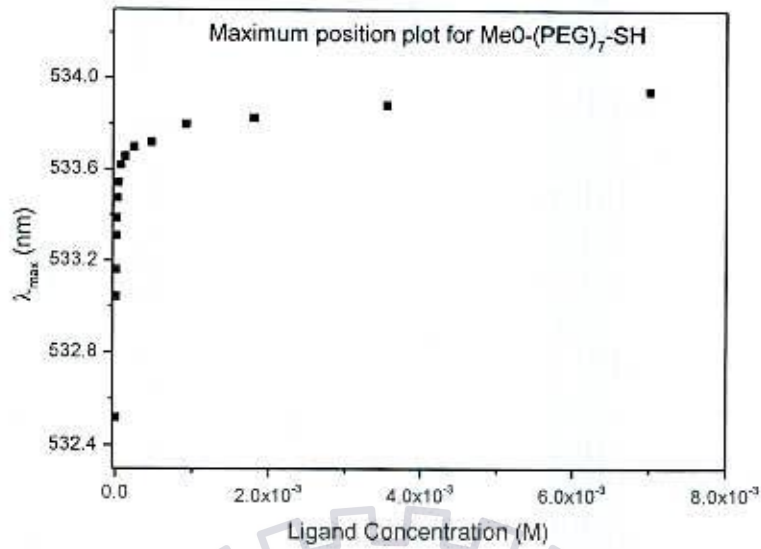


Figure 23: Plot of λ_{max} against ligand conc. for MeO-(PEG)₇-SH modified 60 nm AuNP

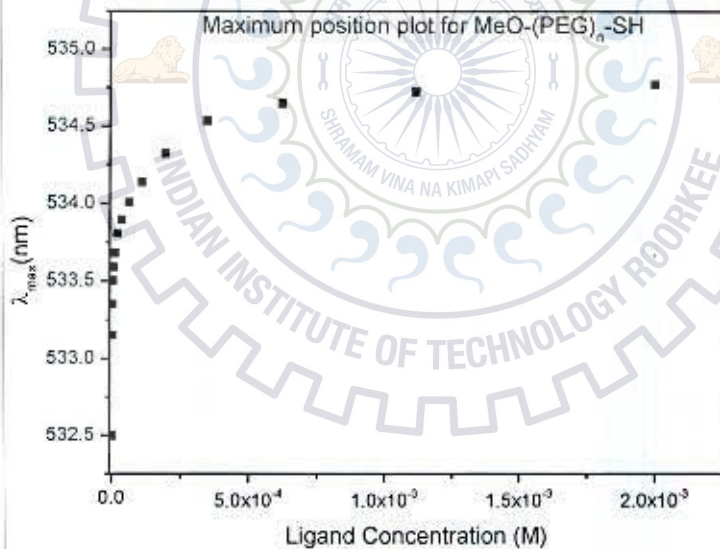


Figure 24: of λ_{max} against ligand conc. for MeO-(PEG)_n-SH modified 60 nm AuNP

MeO-(PEG)_n-SH was then used for surface modification experiments with the 60 nm gold nanoparticles. Fig. 23 which shows the λ_{max} plotted against the solution concentration again shows a plateau region indicating the achievement of gold nanoparticle surface saturation with the thiol ligand. However, a maximum plasmon resonance band shift of 2.3 nm is achieved at the end of the surface modification experiment. This larger shift in plasmon band is due to the fact that the MeO-(PEG)_n-SH ligand has a much longer PEG chain than MeO-(PEG)₇-SH ligand. Therefore, if

even though both the ligands are covalently connected to gold by thiol linkage, the MeO-(PEG)_n-SH ligand has a larger interaction with the nanoparticle owing to the longer PEG chain.

4.3.1.2 Dynamic Light Scattering results

After allowing the samples to equilibrate overnight, the PEGylated gold nanoparticles along with the blank 60 nm gold nanoparticles were measured by dynamic light scattering to determine the changes in their size post surface modification. Table 12 shows the hydrodynamic diameter of all the samples along with their polydispersity index.

Table 12: DLS analysis of PEGylated 60 nm gold nanoparticles

Sample Id	Hydrodynamic diameter (nm)	Polydispersity index
Blank 60 nm AuNP	63.6	0.38
MeO-(PEG) ₇ -SH modified AuNP	71.8	0.31
MeO-(PEG) _n -SH modified AuNP	80.4	0.28

As expected, there is a consistent but small increase in the size of the ligand modified gold nanoparticles with respect to the blank 60 nm AuNPs. Moreover, the MeO-(PEG)_n-SH modified AuNP has a larger hydrodynamic diameter than the MeO-(PEG)₇-SH modified AuNP, owing to its longer PEG chain. It must be kept in mind, that the DLS provides the hydrodynamic diameter and not the physical dimension of the nanoparticles. This hydrodynamic diameter also includes the hydration sphere surrounding the gold nanoparticle. Therefore, the longer the PEG chain, the more hydrophilic character the nanoparticle has. Hence, MeO-(PEG)_n-SH modified AuNP is more solvated than the MeO-(PEG)₇-SH modified AuNP. Consequently it has a larger hydrodynamic diameter.

4.3.1.3 TEM Analysis

It has already been discussed that grafting of PEG chains onto the gold nanoparticles would enhance the stability of the gold nanoparticles. The PEG chains would cause

steric repulsion and reduce the aggregation tendency of gold nanoparticles. To ascertain if the such behavior is shown for our samples, TEM analysis was performed for the ligand modified gold nanoparticles and also the blank 60 nm AuNPs for comparison.

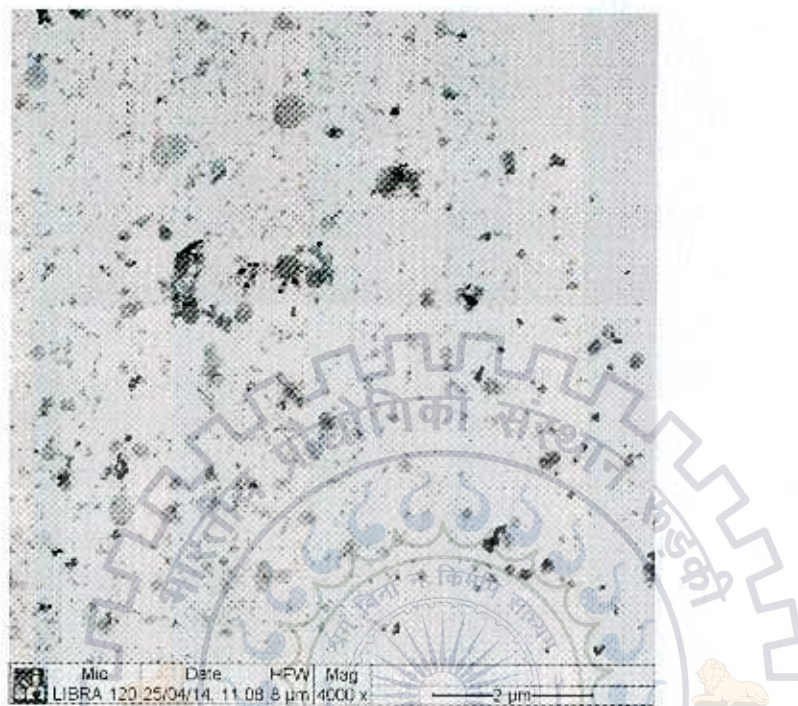


Figure 25: TEM micrograph of 60 nm gold nanoparticles after sonication

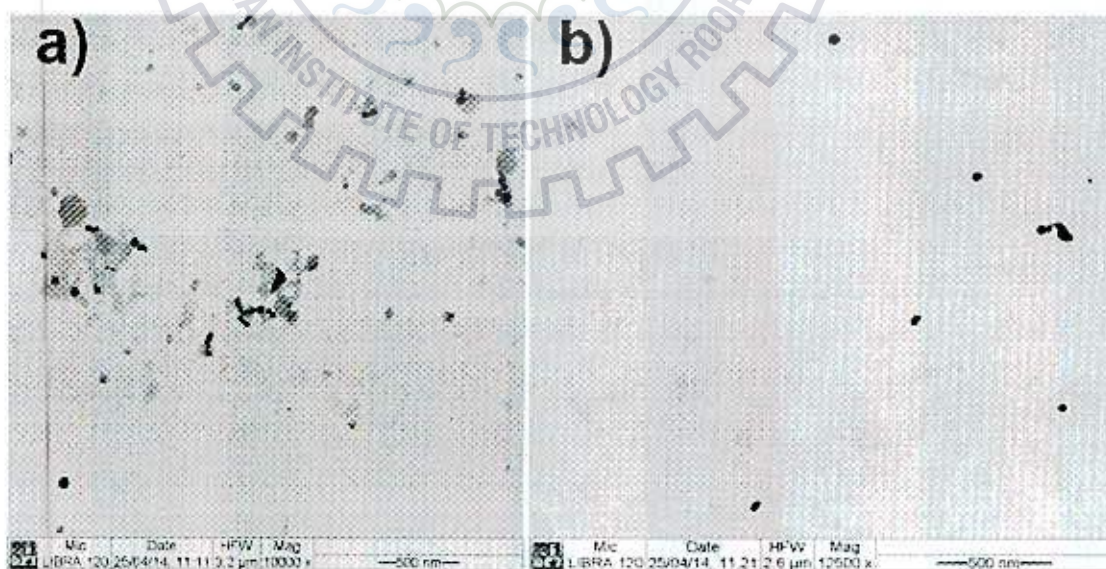


Figure 26: TEM micrograph of 60 nm gold nanoparticles modified with a) MeO-(PEG)₇-SH b) MeO-(PEG)_n-SH after sonication

Fig. 25 shows the TEM micrograph of the blank 60 nm gold nanoparticles after sonication for 5 minutes. Fig. 26a and fig. 26b are TEM micrographs of MeO-(PEG)₇-

SH modified AuNP and MeO-(PEG)_n-SH modified AuNP, respectively after sonication for 5 minutes.

As it can be observed in fig. 25, the gold nanoparticles which are also citrate stabilized, persist in their tendency to aggregate even after sonication. However, in case of fig. 26a, the gold nanoparticles are still closely spaced to each other but there is a lessening of the presence of large aggregates which were seen in fig. 25. Finally in fig. 26a we see gold nanoparticles which are widely spaced apart from each other and uniformly dispersed throughout. Therefore, it can be concluded that as the PEG chain length or molecular weight increases, the steric repulsion between the chains is larger, leading to greater stability of the grafted gold nanoparticles. Therefore, after taking into account the DLS, UV-vis and TEM investigations, it was concluded that the MeO-(PEG)_n-SH ligand would be used for surface modification of the AuNPs. Moreover, the presence of longer PEG chains would also increase the chances of inter-chain digitations between the PEG chains grafted on the AuNP and the PEG chains of the polymersome, to form a PEG-AuNP hybrid system.

4.3.2 Gold nanoparticle uptake by PEG-AuNP hybrid

4.3.2.1 UV-vis spectroscopy results

The MeO-(PEG)_n-SH modified AuNPs were utilised for the investigation of possible PEG-AuNP hybrid structures. In sample SP63, the modified AuNPs were added during polymersome formation, whereas in sample SP76, the modified AuNPs were added to preformed polymersomes. UV-vis analysis was performed for both the samples along with the blank polymersome sample to compare for possible plasmon band shift of the gold nanoparticles, due to aggregation induced by PEG-AuNP hybrid.

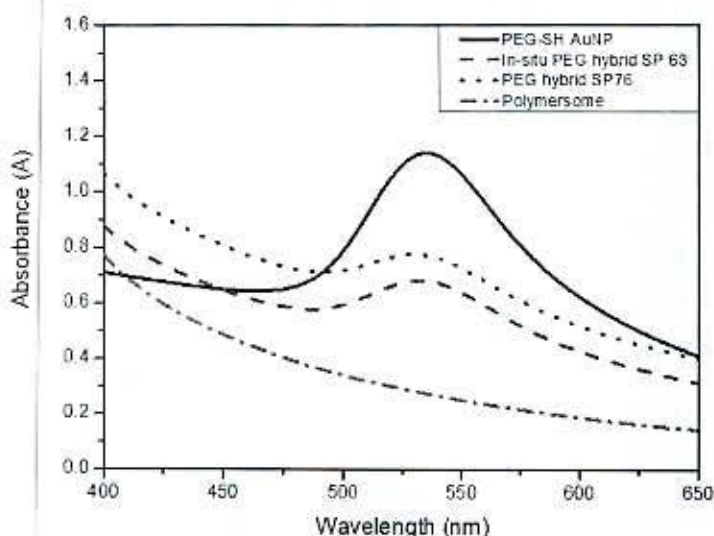


Figure 27: UV-vis spectra of plasmon shift due to PEG-AuNP hybrid

Fig. 27 shows the UV-vis spectra of the samples in the spectral range of 400-650 nm. The shift in the plasmon band of the modified gold nanoparticles after addition to the polymersomes is determined as can be seen from table 13.

In both the samples SP63 and SP76 we see a negative shift in the plasmon band of the gold nanoparticles when compared to the modified AuNPs. The negative shift in the plasmon resonance band means that there is a decrease in wavelength of the absorbed light and a corresponding increase in the frequency. It has been reported that such a negative shift or blue shift is observed in case of either weakly interacting systems or the complete absence of any interactions. In the latter case, the shift may be explained by the change in dielectric constant of the medium surrounding the nanoparticle, which in this case may be due to the presence of polymersomes. Since, UV-vis results do not provide us with a solid reason for the plasmon shifts, the samples were the analysed by DLS to check for any size increase induced by aggregation.

Table 13: UV-vis analysis of plasmon shift due to PEG-AuNP hybrid

Sample Id	Mode of surface modified AuNP addition to polymersome	λ_{\max} (nm)	Shift in λ_{\max} (nm)
MeO-(PEG) _n -SH modified 60 nm AuNP	NA	535.2	NA
SP63	During self-assembly	532.2	-3
SP76	Preformed polymersome	530	-5.2

4.3.2.2 Dynamic Light Scattering Results

The samples SP63, SP76 as well as the blank polymersomes were analysed by dynamic light scattering to investigate the formation of possible PEG-AuNP hybrid structures which would produce an aggregated PEG-AuNP system. Fig. 28 shows the intensity plot versus the hydrodynamic diameter of the measured samples. Table 14 gives the hydrodynamic diameter as well as the polydispersity of each of the samples.

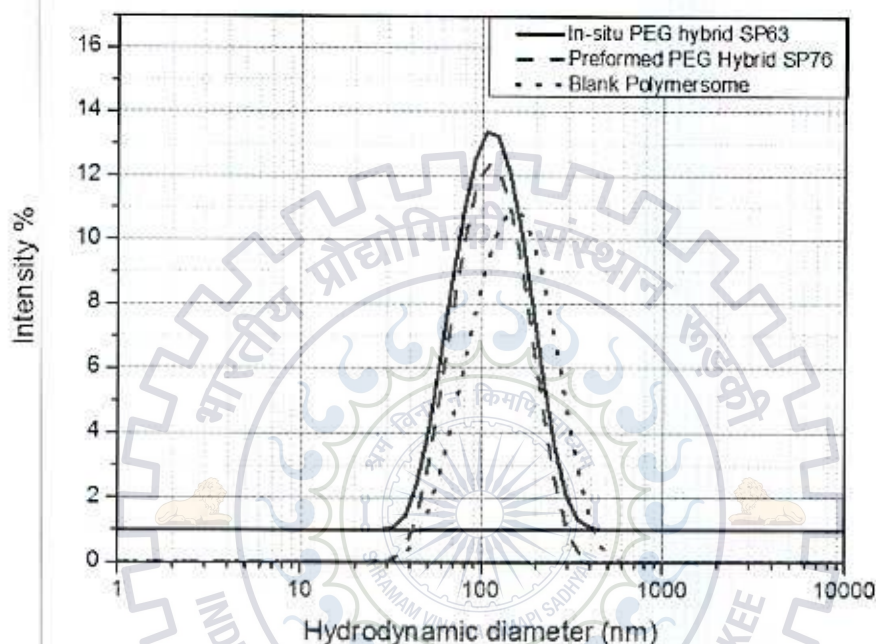


Figure 28: Intensity averaged diameter plot for AuNP PEG hybrid obtained using DLS

Table 14: DLS analysis for PEG-AuNP hybrid

Sample Id	Mode of surface modified AuNP addition to polymersome	Hydrodynamic diameter (nm)	Polydispersity index
Blank polymersome	NA	128.2	0.19
SP63	During self-assembly	89.6	0.26
SP76	Preformed polymersome	99.5	0.32

The SP63 sample has a hydrodynamic diameter smaller than that of the blank polymersomes as we have seen in case of the previous cases of direct encapsulation of the gold nanoparticles. However, surprisingly, even the sample SP76 where the modified gold nanoparticles are added post polymersome self-assembly process, show size reduction. This is interesting because unlike in case of SP63, the size reduction

cannot be accounted for by disruption of the polymersome self-assembly by gold nanoparticle addition. The only possible explanation for this reduction in size might be that the inter chain digitations of the PEG chains has not been successful. To obtain a clear evidence of the PEG chain interaction or their lack thereof, Cryo-TEM analysis was required.

4.3.2.3 Cryo TEM results

Fig. 29 shows the Cryo-TEM image of the sample SP63 where the PEG modified AuNPs were added in-situ during polymersome self-assembly.

The dark spheres marked by blue arrows show the location of the gold nanoparticles on the Cryo-TEM grid and the yellow arrows indicate the humidity contamination of the sample. It is clearly seen that none of the gold nanoparticles present show any proximity to the polymersomes. Moreover, not a single instance was found where there existed any interaction of the gold nanoparticles with the polymersome periphery, which might have been the result of PEG chain entanglements. Neither was there any gold nanoparticle which was completely engulfed by the polymersome. Therefore, it might be safe to state that in spite of PEGylating the AuNPs in the hopes of inducing specific interactions, this attempt has been unsuccessful. A possible explanation for this might be that the critical micellar concentration required for such interchain digitation induced hybrid formation, has not been achieved yet.

Similar Cryo-TEM analysis for the sample SP76 could not be performed due to lack of time. But coupled with the negative plasmon resonance shift by UV-vis analysis, size reduction by DLS investigation and the lack of PEG interchain digitation observed in Cryo-TEM for SP63, it might not be too wrong to assume a similar fate for sample SP76. Hence, investigation of gold nanoparticle uptake using a stronger supramolecular interaction is required. For this purpose, the threading interaction induced inclusion complex between β -cyclodextrin cavities and PEG chains was investigated as the next step.

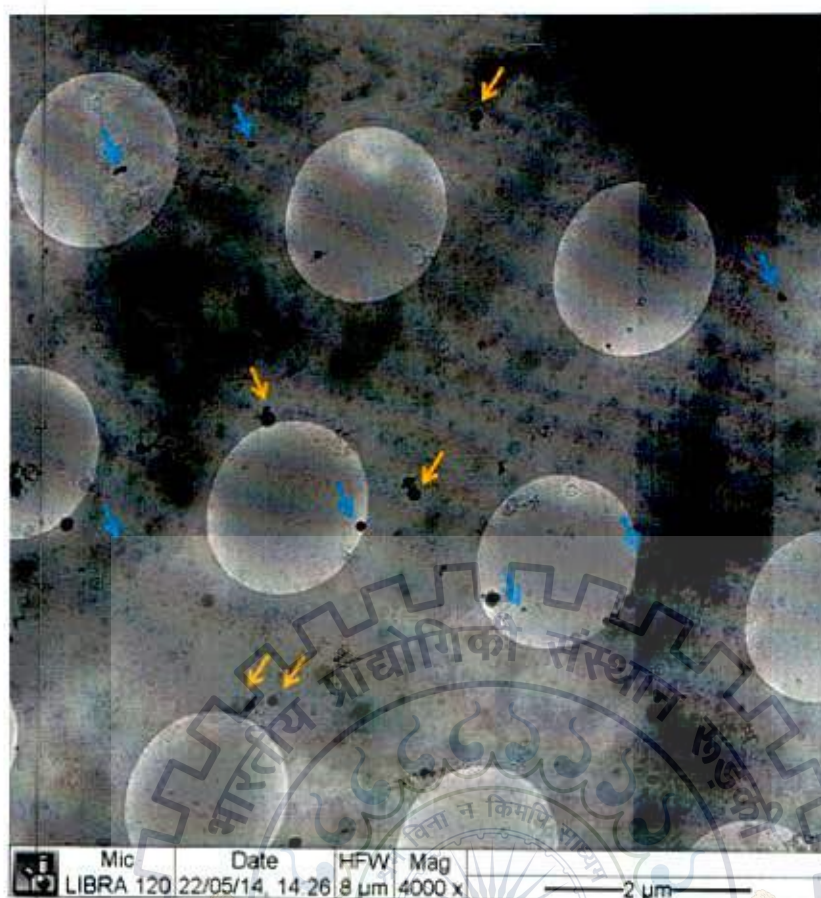


Figure 29: Cryo-TEM micrograph of sample SP63

4.4 Threading interaction between BCD-PEG

As explained in section 3.4, in this approach the surface of the 60 nm gold nanoparticles was first with the two amine-functionalised β -cyclodextrin ligands, CdexB013 and CdexB053. The surface modification experiments were monitored by UV-vis spectroscopy after every ligand titration step.

4.4.1 Surface modification of 60 nm AuNP with β -cyclodextrin ligands

4.4.1.1 UV-vis spectroscopy results

Fig. 30 shows the UV spectra of the 60 nm gold nanoparticles during the surface modification experiment with the 6-Monodeoxy-6-monoamino- β -cyclodextrin [CDexB013] ligand.

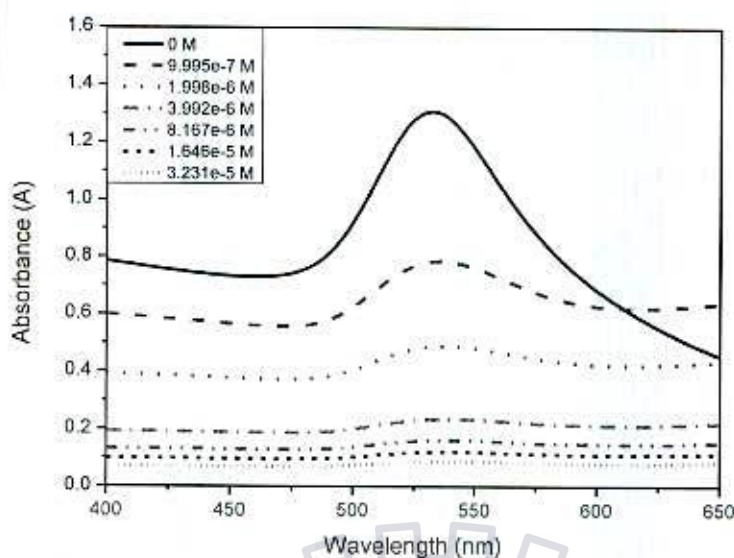


Figure 30: UV-vis spectra of 60 nm AuNP surface modification with CDexB013

A shift in the plasmon resonance band as well as absorbance was noticed after the first titration itself, and the gold nanoparticle solution changed its colour from reddish brown to blue. This in itself indicated a strong shift in the resonance band which can also be seen in fig. 31 which plots the wavelength corresponding to maximum absorbance (λ_{\max}) against the solution concentration. The gold nanoparticle surface was saturated at a concentration lower (8×10^{-6} M) than the calculated theoretical value (3.3×10^{-5} M). This can also be observed in the Fig. 31 where the λ_{\max} attains a maximum value and then flattens into a plateau region finally ending with a dip in the resonance wavelength. At the experimental saturation concentration, a large shift of 9.3 nm in plasmon resonance band of the gold nanoparticles was observed after modification. This indicated a very strong covalent interaction due to the presence of seven amino groups of the β -cyclodextrin ligand with the gold nanoparticles.

Similar surface modification experiments were performed with the mono amino substituted heptakis-(6-amino-6-deoxy)- β -cyclodextrin [CDexB053]. Due to the presence of a single amino group to bind covalently with the gold surface, a weaker plasmon shift was observed. Moreover, there was still an increase in the plasmon resonance band beyond the calculated saturation concentration (2.2×10^{-4} M). This indicated that the complete saturation of the available gold surface had not yet been achieved. Finally, surface modification of the gold nanoparticles with a final ligand

concentration of 8×10^{-4} M yielded a shift of 0.8 nm in the plasmon band, even though saturation had not been reached yet.

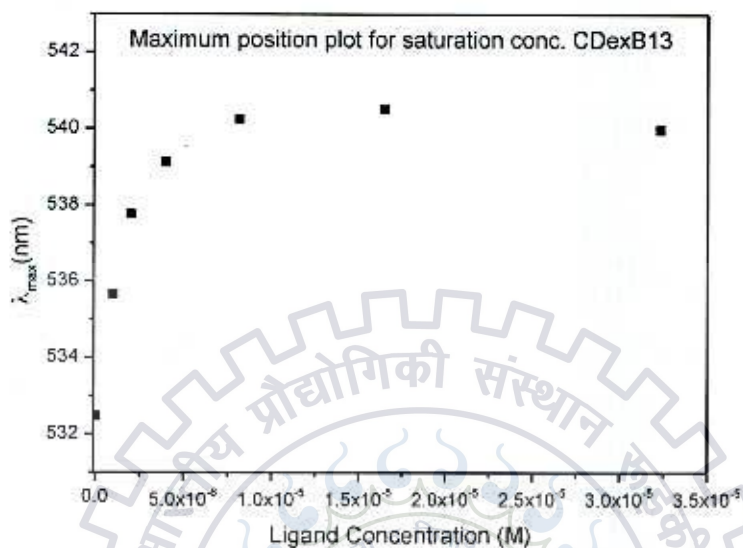


Figure 31: Plot of λ_{max} against ligand conc. for CDexB013 modified 60 nm AuNP

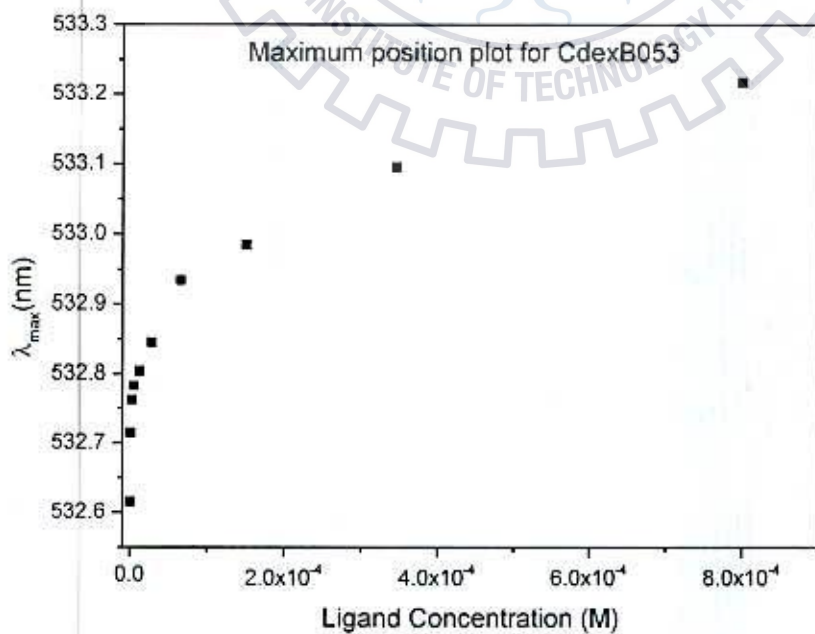


Figure 32: Plot of λ_{max} against ligand conc. for CDexB053 modified 60 nm AuNP

UV-vis spectra of the modified gold nanoparticle solution was measured after overnight equilibration. But no additional plasmon shift was obtained. However surprisingly, the CdexB013 modified gold nanoparticles had formed large aggregates and had precipitated out of the suspension. Dynamic light scattering was employed to investigate the size change in gold nanoparticles caused by surface modification.

4.4.1.2 Dynamic Light Scattering results

The gold nanoparticles modified by both CdexB013 and CdexB053 ligands as well as the blank 60 nm gold nanoparticles were investigated by Dynamic light scattering with parameters as described in section 3.6.1.

Table 15: DLS analysis of β -cyclodextrin-modified 60 nm gold nanoparticles

Sample	Hydrodynamic diameter (nm)	PDI
CdexB013 modified 60 nm AuNP	408.6	0.76
CdexB053 modified 60 nm AuNP	67.8	0.41
60 nm AuNP	63.6	0.38

It is evident from the DLS investigations that the gold nanoparticles after modification with the CdexB013 ligand, that is, the β -cyclodextrin fully substituted with amino groups, causes the gold nanoparticles to form large aggregate which then settle down by precipitating from the suspension. The formation of large clusters was also the reason behind the strong shift in the plasmon resonance band observed during UV-vis investigations. Since, the stability of these gold nanoparticles was compromised, the CdexB013 ligand was deemed unsuitable and the mono substituted CdexB053 ligand was used for further surface modification experiments.

4.4.2 Gold nanoparticle uptake by threading interaction between BCD-PEG

4.4.2.1 UV-vis spectroscopic results

The β CD modified gold nanoparticles were added during polymersome self-assembly for preparation of sample SP62 and in case of sample SP75, they were interacted with preformed polymersomes. UV-vis analysis was performed for these samples to check

for shift in plasmon resonance band of the gold nanoparticle due to possible formation of threading interaction induced inclusion complexes. Fig. 33 shows the UV-vis spectra of these samples and the corresponding plasmon shift values are indicated in table 16.

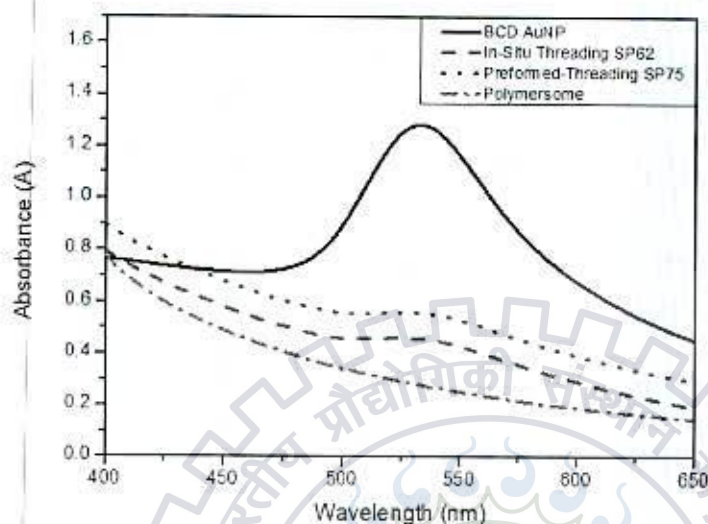


Figure 33: UV-vis spectra of BCD functionalized AuNP- PEG Threading interaction

Table 16: UV-vis analysis of plasmon shift due to threading interaction

Sample Id	Mode of β CD-AuNP addition to polymersome	λ_{\max} (nm)	Shift in λ_{\max} (nm)
β CD modified 60 nm AuNP	NA	533	NA
SP62	During self-assembly	524.7	-8.3
SP75	Preformed polymersome	537	4

For sample SP62 a negative shift in plasmon resonance is observed whereas in case of sample SP75, a positive shift or red shift in plasmon band is observed. As discussed previously, a negative shift in plasmon band most probably means a weakly interacting system or absence of interactions involving ligand on the gold nanoparticle surface. But to eliminate either of the explanations, DLS and Cryo-TEM analysis is required.

Surprisingly for the first time, a positive shift in plasmon resonance is obtained in sample SP75, indicating the presence of specific interactions involving the gold nanoparticles. This shift in the surface plasmon resonance band may be due to the aggregation of the gold nanoparticles to form larger particles or due to the effect of possible interactions on the interface of the gold nanoparticles which cause aggregation. We have already seen that the size of the β CD modified AuNPs is around 68 nm from the DLS investigations which shows that there is no possibility of aggregation due to surface modification. Moreover, previous Cryo-TEM analysis images show that the gold nanoparticles concentration in the polymersome samples is already quite low and that the nanoparticles are uniformly dispersed. These observations therefore discount the possibility that the plasmon shift is due to aggregation of the gold nanoparticles. We are therefore left with the other alternative involving the possibility of aggregation induced by threading interactions involving the β CD that is grafted on the AuNP surface and the PEG chains on the polymersome surface, which causes the positive shift in the plasmon resonance band for sample SP75. Hence, DLS analysis was performed to determine the size distributions of the samples for investigation of possible aggregation by complex formation.

4.4.2.2 Dynamic Light Scattering results

The samples SP62, SP75 along with the blank polymersome samples were analysed by dynamic light scattering using parameters described in section 3.6.1. Fig. 34 shows the intensity plot versus the hydrodynamic diameter of the measured samples. The hydrodynamic diameter of all the samples along with their polydispersity index is provided in table 17.

The DLS results in this case are very interesting because in all our previous DLS investigations of 60 nm AuNP incorporation in polymersomes, we have seen a size reduction in case of the AuNP encapsulated polymersomes. However, this set of DLS results is the first such instance of an increase in size of the AuNP incorporated polymersomes in comparison to the blank polymersomes. Even though, in sample SP62 the increase in size is insignificant, it must be borne in mind that the β CD modified AuNPs have been added in-situ during polymersome formation, which in previous instances has always led to a substantial reduction in size. Combining this with the UV-vis result, we still cannot rule out the possibility of gold nanoparticle

uptake in polymersomes by complex formation. Therefore, investigation of the sample by Cryo-TEM was performed.

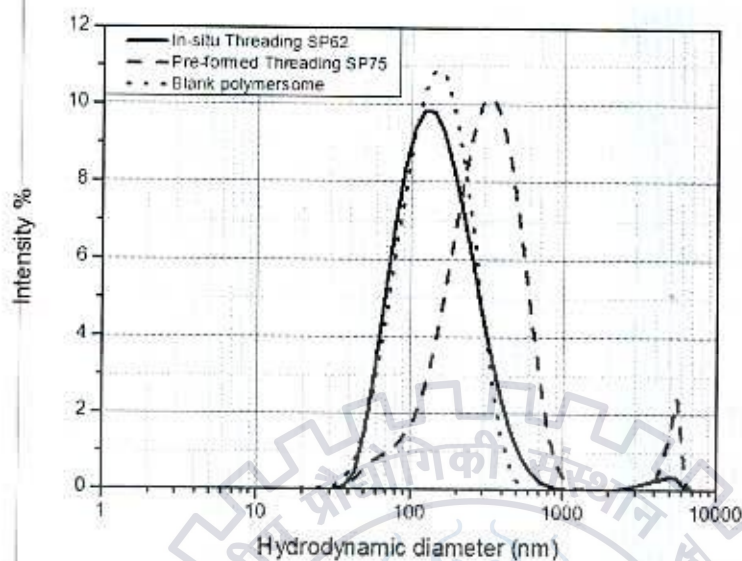


Figure 34: Intensity averaged diameter plot for host-guest complexation polymersome samples

Table 17: DLS analysis for host-guest complexation polymersomes

Sample Id	Mode of β CD-AuNP addition to polymersome	Hydrodynamic diameter (nm)	Polydispersity index
Blank polymersome		128.2	0.19
SP62	During self-assembly	130.7	0.23
SP75	Preformed polymersome	286	0.39

Coming to the case of sample SP75, a huge size increase in size of the sample is observed as compared to the blank polymersomes. The size of this particular species is more than twice that of the regular blank polymersomes. In addition to the strong red shift observed during UV-vis analysis it might be possible that there is indeed the possibility of formation of an inclusion complex due to threading of the PEG chains present on the polymersome, with the β CD cavity.

4.4.2.3 Cryo TEM results

Fig. 35 shows the Cryo-TEM image of the sample SP62 where the β CD modified AuNPs were added in-situ during polymersome self-assembly.

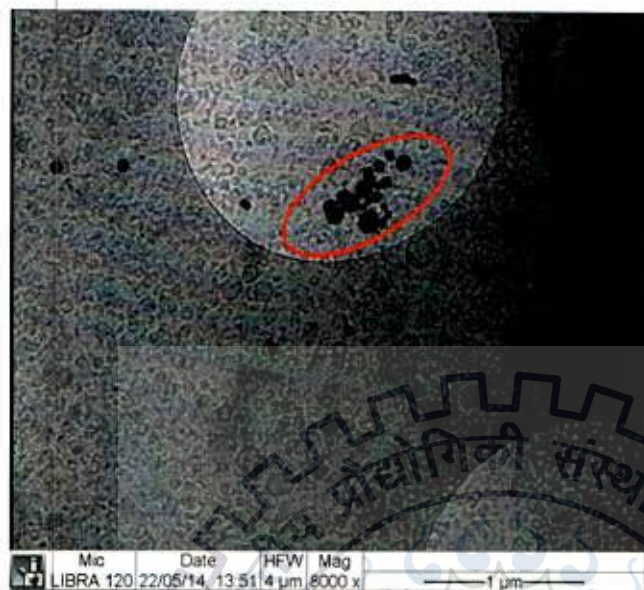


Figure 35: Cryo-TEM micrograph of SP62 for threading interactions

The dark spheres in the image are the 60 nm gold nanoparticles, located on the TEM grid. The polymersomes are visible along with their membrane structure. As can be seen there are a large number of polymersomes throughout the grid. By comparison, there are only a few gold nanoparticles which are dispersed uniformly except for the encircled region. We see a seeming aggregation of gold nanoparticles which are although spaced a little apart from each other. Since, there are a large number of polymersomes, it is difficult to distinguish individual cases of interaction of a single gold nanoparticle with the surrounding polymersomes. However, the arrangement of the gold nanoparticles is quite similar to the expected theoretical model for threading interaction. Therefore, in absence of positive evidence of AuNP-PEG chain interaction, we can only postulate that there is some positive influence due to addition of β CD modified AuNP which balances the possible detrimental effect of the in-situ gold nanoparticle incorporation on polymersome self-assembly.

Due to insufficient time, the Cryo-TEM analysis of sample SP75 could not be performed. But keeping in mind the UV-vis and DLS results it is hypothesised that the β CD forms a dimeric inclusion complex in this case as depicted in fig. 36b, which explains its large size.

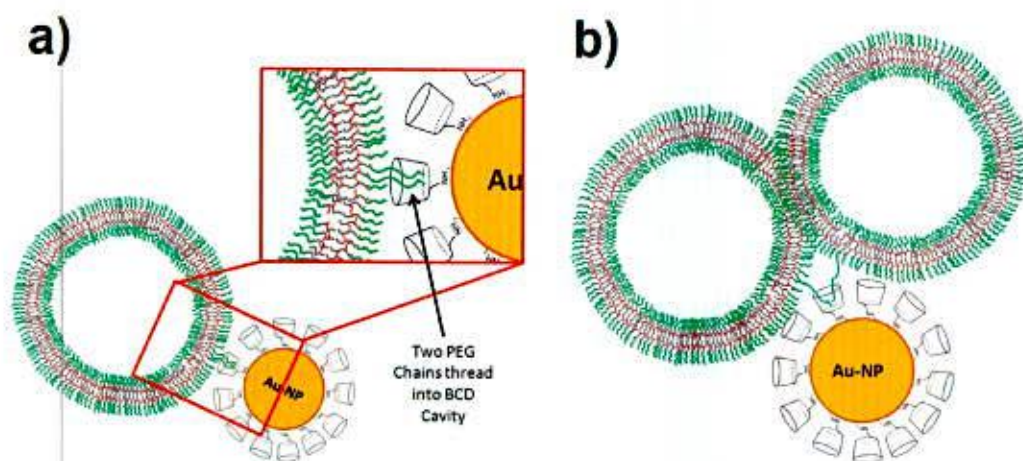


Figure 36: Schematic diagram for formation of a) 1:1 inclusion complex between PEG and β CD b) dimeric(2:1) inclusion complex between PEG and β CD

For the sample SP62, a similar inclusion complex of β CD is proposed with a single polymersome to account for its more moderate size dimension. However, further experiments need to be performed for more concrete evidence in this direction. In spite of it, these results are an important milestone in the course of this study, which show that we have now achieved a basic platform for the gold nanoparticle uptake in polymersomes even with a weak inclusion complex system such as PEG- β CD. Therefore to proceed further in this direction, the last strategy for gold nanoparticle uptake in polymersome, involved the strong host-guest complexation behaviour shown by Adamantane and β CD.

4.5 Gold nanoparticles uptake using host guest chemistry

As explained in section 3.4.3, β CD modified AuNPs were used for host guest interaction with unfunctional BCP and Ada-BCP. Detailed analysis of the β CD modified AuNPs has already been provided in the previous section. Therefore, we will directly focus on the results of the host-guest complexation mechanism.

4.5.1 UV-vis spectroscopic results

The samples SP72, SP73 and SP74 which were prepared by adding the β CD modified AuNPs to preformed Ada-polymsomes and the sample SP61 prepared by in-situ addition of modified AuNP during polymersome formation were analysed by UV-vis spectroscopy to check for possible shift in the plasmon resonance band of the gold nanoparticles due to host-guest interactions.

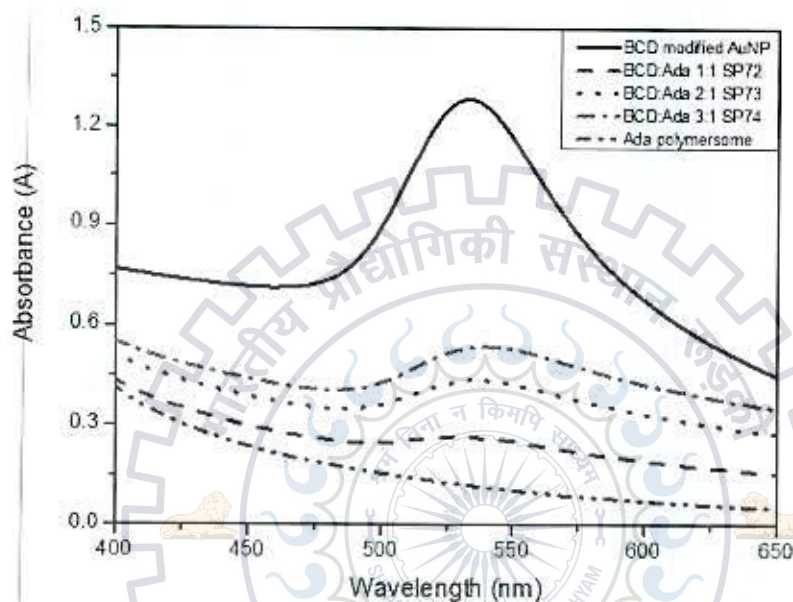


Figure 37: UV-vis spectra of plasmon shift due to host-guest complexation

Table 18: UV-vis analysis of plasmon shift due to host-guest complexation

Sample Id	β CD:Ada molar ratio	Mode of β CD-AuNP addition to polymersome	λ_{\max} (nm)	Shift in λ_{\max} (nm)
β CD modified 60 nm AuNP	-	-	533	-
SP61	3:1	During self-assembly	526	-7
SP72	1:1	Preformed polymersome	529.5	-3.5
SP73	2:1	Preformed polymersome	536.8	3.8
SP74	3:1	Preformed polymersome	539.8	6.8

It can be noted from fig. 37 that there is a clear decrease in the absorbance at λ_{\max} along with a shift in the wavelength at which the absorbance is maximum, which becomes

more pronounced with an increase in β CD content. The table 18 shows the shift in the plasmon band observed in case of each of the samples.

In the samples when β CD modified AuNP is added to preformed Ada-polymerosomes, it is seen that for a 1:1 β CD:Ada molar ratio, there is a negative plasmon shift or a blue shift (shift to shorter wavelengths). But as the β CD:Ada molar ratio increases a positive shift or red shift is noticed in the plasmon resonance band. An increased amount of β CD causes stronger shift in the plasmon band. Moreover, in the case of in-situ addition of β CD modified AuNP during self assembly of Ada-polymerosomes, a negative shift in plasmon resonance is observed. These shifts in the surface plasmon resonance band may be due to the aggregation of the gold nanoparticles to form larger particles or due to the effect of possible interactions on the interface of the gold nanoparticles which cause aggregation. We have already seen that the size of the β CD modified AuNPs is around 68 nm from the DLS investigations which shows that there is no possibility of aggregation due to surface modification. Moreover, previous Cryo-TEM analysis images show that the gold nanoparticles concentration in the polymerosome samples is already quite low and that the nanoparticles are uniformly dispersed. These observations therefore discount the possibility that the plasmon shift is due to aggregation of the gold nanoparticles. We are therefore left with the other alternative involving the possibility of aggregation induced by host-guest interactions involving the β CD that is grafted on the AuNP surface and the Adamantane moieties on the polymerosome surface, which causes the positive shift in the plasmon resonance band for samples SP73 and SP74. The positive plasmon band shift to a longer wavelength reflects the presence of less energetic electrons or a diminishing electron density due to particular aggregation. Therefore, it can be said that the onset of host-guest complexation induces aggregation which causes a red shift due to a decrease in electron density. But for the samples SP61 and SP72, the negative shift or blue shift it cannot be said that there is an absence of host-guest interaction. It has been reported that in certain cases where there is existence of weaker interactions, the system undergoes a blue shift. Therefore, we cannot completely discount the possibility of host-guests in these two cases. Hence, DLS investigations were performed to determine the size distributions of the samples.

4.5.2 Dynamic Light Scattering results

The samples SP61, SP72, SP73, SP74 and the blank Ada-polymerosomes were analysed by dynamic light scattering with the same parameters for polymerosomes as described in section 3.6.1.

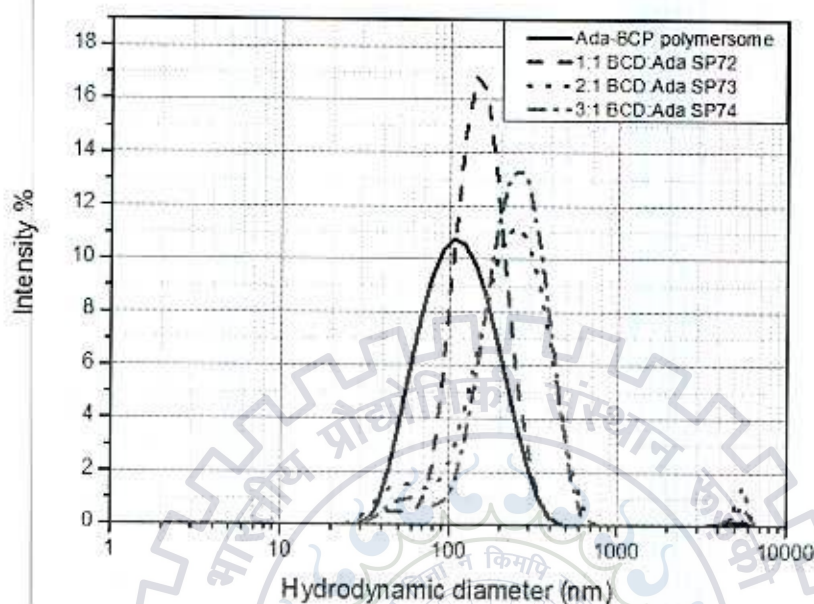


Figure 38: Intensity averaged diameter plot for host-guest complexation polymerosome samples

The hydrodynamic diameter of all the samples along with their polydispersity index is provided in table 19.

In all our previous DLS investigations of 60 nm AuNP incorporation in polymerosomes, we have seen a size reduction in case of the AuNP encapsulated polymerosomes. However, in this case, all the samples including sample SP61, where the β CD modified AuNP is added during the self-assembly process of the polymerosomes, show a significant increase in size. This result most definitely points a positive influence or interaction even during the self-assembly process which encourages the AuNP to stay in the vicinity of the polymerosome in spite of our earlier postulation that AuNP addition harms self assembly process. A similar trend relating to increased size is observed in all the samples SP72, SP73 and SP74. Moreover, there is clear increase in size of the polymerosomes with an increase in the β CD:Ada molar ratio. Therefore, it might be said that there is a formation of host-guest complexes between β CD grafted on AuNP and Adamantane moieties on the polymerosome periphery. This means that there is an uptake of gold nanoparticles by the polymerosome on its periphery leading to larger sized AuNP-polymerosome

complexes. Additionally an increase in the β CD amounts leads to increasing host-guest complexation and hence, even bigger AuNP-polymersome structures. Moreover, an increase in the polydispersity index was also observed in all the cases when compared to the blank Ada-polymersome.

Table 19: DLS analysis for host-guest complexation polymersomes

Sample Id	β CD:Ada molar ratio	Mode of β CD-AuNP addition to polymersome	Hydrodynamic diameter (nm)	Polydispersity index
Blank Ada-polymersome	NA	NA	102.4	0.19
SP61	3:1	During self-assembly	143.5	0.20
SP72	1:1	Preformed polymersome	178.3	0.31
SP73	2:1	Preformed polymersome	204.5	0.44
SP74	3:1	Preformed polymersome	248.8	0.40

4.5.3 Cryo-TEM results

For conclusive evidence of gold nanoparticle uptake in polymersomes by host-guest complexation, Cryo-TEM analysis was performed for sample SP61.

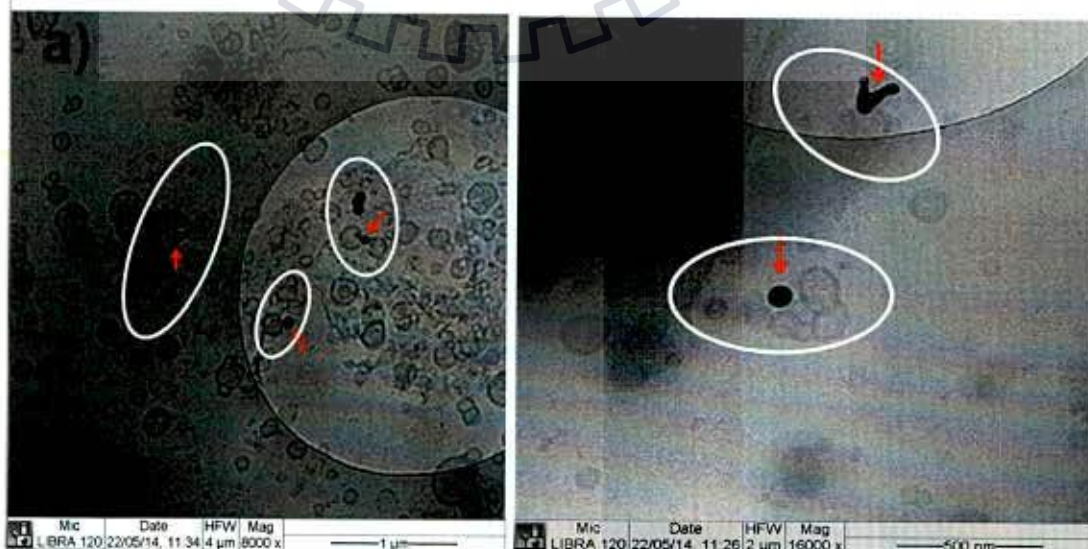


Figure 39 a) & b): Cryo-TEM micrographs of SP61 showing host-guest complexation

As can be seen in fig. 39a, the encircled regions are of interest to investigate the uptake of gold nanoparticles by the polymersomes. The red arrows point to the gold nanoparticles which can be seen as having clear interactions with the polymersome periphery. A single AuNP is shown interacting with the outer shell of at least 1 or 2 polymersomes.

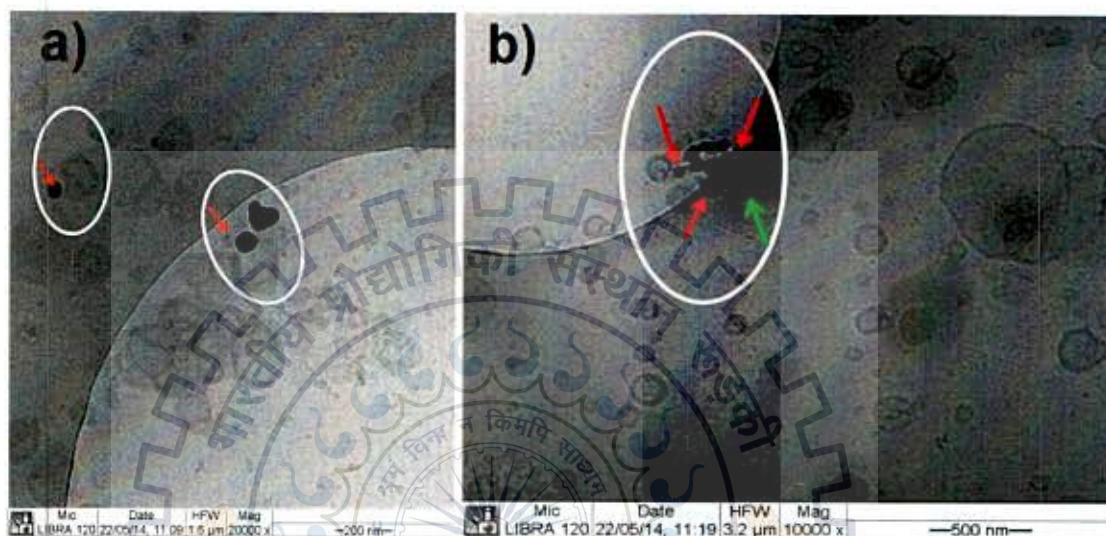
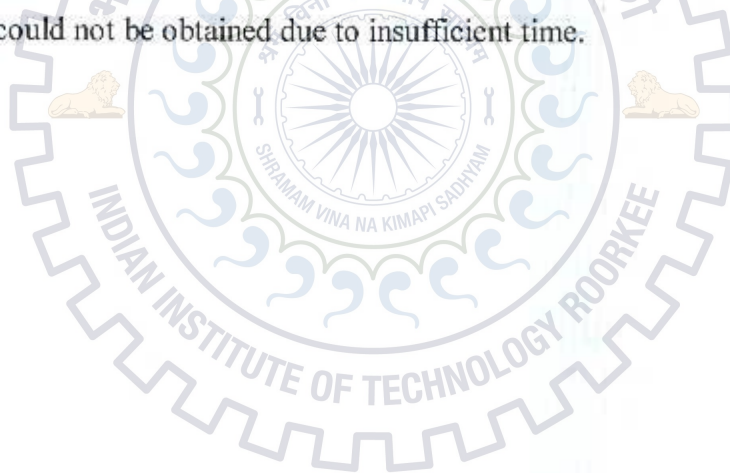


Figure 40 a) & b) Cryo-TEM micrograph of SP61 for host-guest complexation

Similarly, Fig. 39b shows a single AuNP interacting with the periphery of a number of polymersomes, which form a cluster around it. Likewise, in fig. 40a the encircled regions show further instances of AuNP-polymersome peripheral interaction.

Fig. 40b is also interesting because the gold nanoparticle marked with a green arrow looks to be encapsulated within the interior cavity of the polymersome. This is possibly the sole instance where we have noticed complete engulfment of a 60 nm gold nanoparticle within a polymersome. In the same figure, we also see other gold nanoparticles which are marked in red interacting with the polymersome periphery. Such instances of AuNP-polymersome aggregation had not been noticed in any of the previous Cryo-TEM analyses for the 60 nm AuNPs, where we had rare examples of interaction between a single gold nanoparticle with a single polymersome. Therefore, from the above images, it can be conclusively stated that there is a marked interaction between the gold nanoparticles and the outer shell of the polymersomes. This interaction can now be positively attributed to the host-guest complexation between the β CD grafted onto the gold nanoparticle and the Adamantane moieties that are exposed on the outer shell of the polymersome structure.

Keeping in mind the negative plasmon shift from the UV-vis results which suggest a mild host-guest interaction and the size increase seen by DLS investigations, there are a number of instances of AuNP-polymerosome peripheral interaction. Therefore, it can be said that even with in-situ addition of the modified AuNPs, there is successful uptake of the gold nanoparticles by the polymerosomes due to host-guest complexation. Hence, it would be logical to expect even better host-guest complexation induced aggregation between AuNPs and polymerosomes for the other samples, that is, SP72, SP73 and SP74. These samples have already shown better plasmon band shifts in UV-vis investigation and larger sized polymerosome entities in DLS characterisation. Moreover, these samples have the added advantage that the modified AuNPs have been added to pre-formed polymerosomes. Therefore, the chance of detrimental effect to polymerosome self-assembly has already been eliminated along with the possibility of complete encapsulation of any AuNPs within the internal hydrophilic cavity of the polymerosomes. However, positive confirmation by Cryo-TEM analysis for these samples could not be obtained due to insufficient time.



5 Conclusion

Encapsulation of small sized (1-10 nm) gold nanoparticles in polymersomes had already been studied extensively by researchers. With the aid of surface coatings to create hydrophobic-hydrophilic interactions, the location of incorporation of the gold nanoparticles within the polymersome can also be guided. However, incorporation of large sized (beyond 20 nm) gold nanoparticles in polymersomes has been relatively unexplored. Although large sized gold nanoparticles demonstrate enhanced optical properties which can be harnessed for bio-medical applications, the large size seriously compounds the problems faced during encapsulation of even smaller sized gold nanoparticles. The scope of this thesis was to determine the possibility of uptake of the larger sized gold nanoparticles (30 nm and 60 nm) by the polymersomes. pH responsive polymersomes with hydrodynamic diameter ranging from 110-140 nm were used to perform these encapsulation studies.

For initial investigations relating to the encapsulation of pre-formed gold nanoparticles within pH responsive polymersomes, 12 nm gold nanoparticles were employed. An in-situ or direct encapsulation protocol was designed wherein the gold nanoparticles were introduced into the block polymer solution at pH 5, followed by subsequent pH increase to aid in self-assembly of polymersomes. Although this direct encapsulation method was successful in the case of 12 nm AuNP, similar experiments with the 30 nm and 60 nm citrate stabilised AuNPs demonstrated poor encapsulation efficiency.

DLS analysis of both the 30 nm and the 60 nm gold nanoparticle encapsulated polymersomes showed a significant size reduction when compared to the blank polymersomes, unlike that for the 12nm AuNP. Cryo-TEM investigations for the 30 nm AuNPs, revealed that there were few cases of completely internalised AuNPs and slightly more cases of partial engulfment by the polymersome. Moreover, with an increase in the AuNP:BCP molar ratio there was an improvement in the encapsulation mechanism. But this avenue could be investigated more extensively because the concentration of the stock solution of the AuNP sol was quite low to begin with. Similar Cryo-TEM investigations for the 60 nm AuNP encapsulated polymersomes, revealed a complete absence of wholly internalised gold nanoparticles. There were also very few instances of AuNPs interacting with the polymersome by partial engulfment. It was therefore evident that size of the gold nanoparticles was an

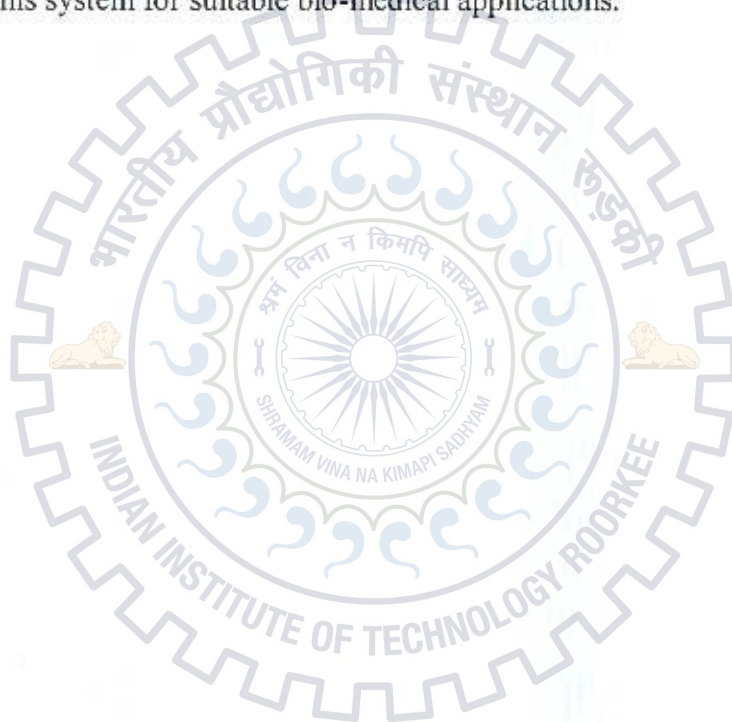
important factor in determining the encapsulation efficiency. Moreover, it is postulated that in-situ addition of the gold nanoparticles might be detrimental to the polymersome self-assembly to explain the size reduction of the polymersomes. Much is still not understood about the nanoparticle incorporation mechanism in polymersomes along with the self-assembly process governing polymersome formation. But such an investigation is beyond the scope of this research.

To improve the chances of nanoparticle uptake in polymersomes, specific interactions involving introduction of guiding ligands were employed. The first strategy in this direction was investigating the formation of PEG-AuNP hybrid caused by inter chain digitations between PEGylated AuNP and PEG chains on polymersomes. Modified AuNPs were added both in-situ and also to pre-formed polymersomes. But, subsequent investigations by DLS, UV-vis and Cryo-TEM revealed that the formation of the proposed hybrid was unsuccessful. This might be because the critical micellar concentration required for this structure has not been attained yet even though the gold nanoparticle surface had been completely saturated with PEG ligands.

Therefore, supramolecular chemistry of threading interactions between PEG chains of the polymersome and the cavity of β -Cyclodextrin grafted on AuNP was used for investigating the formation of a possible inclusion complex which would enable gold nanoparticle uptake. In case of the in-situ prepared polymersomes, although there was a size increase in DLS analysis, Cryo-TEM could not positively confirm the formation of an inclusion complex. However, significant size increase in DLS and a strong red shift in plasmon band by UV-vis analysis for pre-formed polymersomes show promising results prompting the possibility of a formation of a postulated dimeric complex. Cryo-TEM analysis of this sample will be performed for concrete evidence of such a complex and subsequently induced nanoparticle uptake.

Lastly, the strong host-guest complexation behaviour exhibited by Adamantane and β -Cyclodextrin was utilised for selective uptake of the gold nanoparticles by polymersomes. By far, the results of this strategy have been the most encouraging. Size increase was observed in DLS analysis of both the in-situ and pre-formed polymersome samples. Moreover, increased β -CD:Ada molar ratio showed a concurrent trend of increased hydrodynamic diameter. UV-vis analysis also showed first a blue shift and then an increasing red shift in plasmon band further solidified the

possibility of host-guest interactions. Finally, Cryo-TEM analysis of the in-situ polymersome-AuNP sample, revealed the first instance of a 60 nm AuNP completely encapsulated within the hydrophilic internal cavity of the polymersome. Numerous instances of AuNP interaction with the periphery of a single or multiple polymersomes could also be observed. This completely supports the DLS and UV-vis results thereby indicating the formation a host-guest complex between the polymersome surface and the gold nanoparticle. Therefore, host-guest complexation induced gold nanoparticle uptake provided the most promising route to achieve the objective of this study. With the successful establishment of this method for uptake of large sized gold nanoparticles by polymersomes, subsequent investigations can now be undertaken to modify this system for suitable bio-medical applications.



References

1. *Gold nanoparticles: Optical properties and implementations in cancer diagnosis and photothermal therapy.* **El-Sayed, Xiaohua Huang and Mostafa A.** 2010, Journal of Advanced Research.
2. *Functionalized Gold Nanoparticles and Their Biomedical Applications.* **Pooja M. Tiwari, Komal Vig, Vida A. Dennis and Shree R. Singh.** s.l. : Nanomaterials, 2011.
3. *Gold Nanoparticles: Assembly, Supramolecular Chemistry, Quantum-Size-Related Properties, and Applications toward Biology, Catalysis, and Nanotechnology.* **Astruc, Marie-Christine Daniel and Didier.** s.l. : Chem. Rev., 2004.
4. *Self-Assembled Plasmonic Vesicles of SERS-Encoded Amphiphilic Gold Nanoparticles for Cancer Cell Targeting and Traceable Intracellular Drug Deliver.* **Jibin Song, Jiajing Zhou and Hongwei Duan.** s.l. : Journal of the American Chemical Society, 2012.
5. *Advances and challenges in smart and functional polymer vesicles.* **O'Reilly, Jianzhong Du and Rachel K.** s.l. : Soft Matter, 2009.
6. *Size Selective Incorporation of Gold Nanoparticles in Diblock Copolymer Vesicle Wall.* **Jiangping Xu, Yuanyuan Han, Jie Cui, and Wei Jiang.** s.l. : Langmuir, 2013.
7. *Gold nanoparticles in biomedical applications: recent advances and perspectives.* **Khlebtsov, Lev Dykman and Nikolai.** s.l. : Chem. Soc. Rev., 2011.
8. *Experimental Relations of Gold (and other Metals) to Light.* **Faraday, M.** s.l. : Philos. Trans. R. Soc. London, 1857.
9. *Colloidal metals: past, present and future.* **Thomas, John M.** s.l. : Pure & Appl. Chem, 1988.
10. *An immunocolloid method for the electron microscope.* **Taylor, W. P, Faulk and G. M.** s.l. : Immunochemistry, 1971.
11. *Large Clusters and Colloids.* **Schmid, G.** s.l. : Chem. Rev., 1992.
12. *From Monolayers to Nanostructured Materials: An Organic Chemist's View of Self-Assembly.* **Bethell, D., et al.** s.l. : J. Electroanal. Chem., 1996.
13. *A study of nucleation and growth processes in the synthesis of colloidal gold.* **Turkevich J., Stevenson P.C. and Hillier J.** s.l. : Discuss. Faraday Soc., 1951.
14. *Size Correlation of Optical and Spectroscopic Properties for Gold Nanoparticles.* **Peter N. Njoki, I-Im S. Lim, Derrick Mott, Hye-Young Park, Bilal Khan, Suprav Mishra, Ravishanker Sujakumar, Jin Luo, and Chuan-Jian Zhong.** 2007, J. Phys. Chem. C.
15. *Metal clusters in chemistry.* **U. Simon, in P. Braunstein, C. A. Oro, P. R. Raithby (Eds.):.** 1999, Wiley VCH.
16. *Handbook of surface plasmon resonance.* **Richard B. M. Schasfoort, Anna J. Tudos.** pp. 31-35.
17. *Preparation of colloidal gold.* **M., Faraday.** 1857, Philos Trans.
18. *Ultraviolet-visible absorption.* **D.G., Creighton J.A. and Eadon.** 1991, J Chem Soc Farad.

19. **Conde, João Diogo Osório de Castro.** *Cancer theranostics: multifunctional gold nanoparticles for diagnostics and therapy.* s.l. : University of Lisbon, 2013.
20. *Optical Antennas.* **Palash Bharadwaj, Bradley Deutsch, and Lukas Novotny.** 2009, Advances in Optics and Photonics.
21. *Controlling the surface enhanced Raman effect via the nanoshell geometry.* **J. Jackson, S. Westcott, L. Hirsch, J. West, and N. Halas.** 2003, Appl. Phys.Lett.
22. *A hybridization model for the plasmon response of complex nanostructures.* **E. Prodan, C. Radloff, N. J. Halas, and P. Nordlander.** 2003, Science.
23. *Injectable nanomaterials for drug delivery: Carriers, targeting moieties, and therapeutics.* **David M. Webster, Padma Sundaram , Mark E. Byrne.** 2012, European Journal of Pharmaceutics and Biopharmaceutics.
24. *The first targeted delivery of siRNA in humans via a selfassembling, cyclodextrin polymer-based nanoparticle: from concept to clinic.* **Davis, M E.** 2009, Molecular Pharmaceutics.
25. *PEGylation, successful approach to drug delivery.* **F.M. Veronese, G. Pasut.** 2005, Drug Discovery Today.
26. *In vivo tumor targeting and spectroscopic detection with surface-enhanced Raman nanoparticle tags.* **Ximei Qian, Xiang-Hong Peng, Dominic O Ansari, Qiqin Yin-Goen, Georgia Z Chen, Dong M Shin, Lily Yang, Andrew N Young, May D Wang & Shuming Nie.** 2007, Nature Biotechnology.
27. *Depth resolved photothermal OCT detection of macrophages in tissue using nanorose.* **A. S. Paranjape, R. Kuranov, S. Baranov et al.** 2010, Biomedical Optics Express.
28. *Photoacoustic tomography of a nanoshell contrast agent in the in vivo rat brain.* **Y. Wang, X. Xie, X. Wang et al.** 2004, Nano Letters.
29. *Gold nanoparticles: interesting optical properties and recent applications in cancer diagnostics and therapy.* **Xiaohua Huang, Prashant K Jain, Ivan H El Sayed, Mostafa A El Sayed.** 2007, Future medicine.
30. *Heparin immobilized gold nanoparticles for targeted detection and apoptotic death of metastatic cancer cells.* **Lee, K., et al.** 2010, Biomaterial.
31. *Gold Nanoparticles in Biology: Beyond Toxicity to Cellular Imaging.* **Catherine J Murphy, Anand M Gole, John W Stone, Patrick N Sisco, Alaaldin M Alkilany, Edie C Goldsmith and sarah C Baxter.** 2008, Accounts of Chemical Research .
32. *PEG-Modified Gold Nanorods with a Stealth Character for in Vivo Applications.* **Niidome, T., et al.** s.l. : J. Controlled Release, 2006.
33. *Preparation of Functionally PEGylated Gold Nanoparticles with Narrow Distribution through Autoreduction of Auric Cation by r-Biotinyl-PEG-block-[poly(2 (N,N-dimethylamino)ethyl methacrylate)].* **Takehiko Ishii, Hidenori Otsuka, Kazunori Kataoka, and Yukio Nagasaki.** s.l. : Langmuir, 2004.
34. *Synthetic Bio-nanoreactor: Mechanical and Chemical Control of Polymersome Membrane Permeability.* **Jens Gaitzsch, Dietmar Appelhans, Linge Wang, Giuseppe Battaglia, and Brigitte Voit.** s.l. : Angew. Chem. Int. Ed., 2010.

35. *Vectorial budding of vesicles by asymmetrical enzymatic formation of ceramide in giant liposomes.* **P. K. J. Kinnunen, J. M. Holopainen and M. I. Angelova.** s.l. : *Perspect. Supramol. Chem.*, 2000.
36. *Stimuli-Responsive Polymersomes for Programmed Drug Delivery.* **Fenghua Meng, Zhiyuan Zhong, and Jan Feijen.** s.l. : *Biomacromolecules*, 2009.
37. *Photo-crosslinked and pH sensitive polymersomes for triggering the loading and release of cargo.* **Jens Gaitzsch, Dietmar Appelhans, David Grafe, Petra Schwille and Brigitte Voit.** s.l. : *Chem. Commun.*, 2011.
38. *Stimuli-responsive polypeptide vesicles by conformation-specific assembly.* **Bellomo E.G., Wyrsta M.D., Pakstis L, Pochan D.J., Deming T.J.** s.l. : *Nat Mater.*, 2004.
39. *Release from Polymeric Vesicles in Blood Plasma and PVA Hydrogel.* **Litvinchuk, S., et al.** s.l. : *Pharm. Res.*, 2009.
40. *Stimuli- Responsive Polymersomes as Nanocarriers for Drug and Gene Delivery.* **Onaca, O., et al.** s.l. : *Macromol. Biosci.*, 2009.
41. *Preparation of Block Copolymer Vesicles in Solution.* **Patrick Lim Soo, Adi Eisenberg.** s.l. : *Journal of Polymer Science: Part B: Polymer Physics*, 2004.
42. *Slow Relaxation Dynamics of Tubular Polymersomes after Thermal Quench.* **Reinecke, A. A. and Doebereiner, H.-G.** s.l. : *Langmuir*, 2003.
43. *Biocompatible Polymer Vesicles from Amphiphilic Triblock Copolymers and Their Interaction with Bovine Serum Albumin.* **A. Wittemann, T. Azzam and A. Eisenberg.** s.l. : *Langmuir*, 2007.
44. *Spontaneous Formation of Vesicles by Self-Assembly of Cationic Block Copolymer in the Presence of Anionic Surfactants and Their Application in Formation of Polymer Embedded Gold Nanoparticles.* **Rakesh Banerjee, Sujan Dutta, Souvik Pal, and Dibakar Dhara.** s.l. : *J. Phys. Chem. B*, 2013.
45. **Israelachvili, J.** *Intermolecular and Surface Forces.* s.l. : *Academic Press*, 1991.
46. *Morphogenic effect of solvent on crew-cut aggregates of amphiphilic diblock copolymers.* **Y. Yu, L. Zhang and A. Eisenberg.** s.l. : *Macromolecules*, 1998.
47. *Vesicles and Liposomes: A Self-Assembly Principle Beyond Lipids.* **Förster, M. Antonietti and S.** s.l. : *Adv. Mater.*, 2003.
48. *Density functional simulation of spontaneous formation of vesicle in block copolymer solutions.* **Uneyama, T.** s.l. : *J. Chem. Phys.*, 2007.
49. **Doebereiner, P. G. Petrov and H.-G.** *Perspectives in Supramolecular Chemistry: Giant Vesicles.* s.l. : *John Wiley & Sons, Ltd*, 2007.
50. *Thermally responsive vesicles and their structural locking through polyelectrolyte complex formation.* **Y. Li, B. Lokitz and C. L. McCormick.** s.l. : *Angew. Chem., Int. Ed.*, 2006.
51. *Preparation and pH triggered inversion of vesicles from poly(acrylic acid)-block-polystyrene-block-poly(4-vinyl pyridine).* **Liu F, Eisenberg A.** s.l. : *J Am Chem Soc.*, 2003.
52. *pH-Responsive Vesicles Based on a Hydrolytically Self-Cross-Linkable Copolymer.* **Armes, Jianzhong Du and Steven P.** s.l. : *J Am Chem Soc.*, 2005.

53. *Cellular Interactions with Photo-Cross-Linked and pH-Sensitive Polymersomes: Biocompatibility and Uptake Studies.* **Jens Gaitzsch, Irene Canton, Dietmar Appelhans, Giuseppe Battaglia, and Brigitte Voit.** s.l. : Biomacromolecules, 2012.
54. *pH-Dependent Release of Doxorubicin from Fast Photo-Cross-Linkable Polymersomes Based on Benzophenone Units.* s.l. : Chem. Eur. J., 2012.
55. *Formation of liquid core-polymer shell microcapsules.* **Routh, H. N. Yow and A. F.** s.l. : Soft Matter, 2006.
56. *Guiding the location of nanoparticles into vesicular structures: a morphological study.* **Wolfgang H. Binder, Robert Sachsenhofer, Dominique Farnika and Dieter Blaas.** s.l. : Phys. Chem. Chem. Phys., 2007.
57. *Soft Vesicles in the Synthesis of Hard Materials.* **Renhao Dong, Weimin Liu, AND Jingcheng Hao.** s.l. : Accounts of Chemical Research , 2012.
58. *pH-Sensitive Vesicles Based on a Biocompatible Zwitterionic Diblock Copolymer.* **Jianzhong Du, Yiqing Tang, Andrew L. Lewis, and Steven P. Armes.** s.l. : JACS, 2005.
59. *Guiding the location of nanoparticles into vesicular structures: a morphological study.* **Wolfgang H. Binder, Robert Sachsenhofer, Dominique Farnik and Dieter Blaas.** s.l. : Physical Chemistry Chemical Physics, 2007.
60. *Electrochemical Properties of a Boron-Doped Diamond Electrode Modified with Gold/Polyelectrolyte Hollow Spheres.* **Min Wei, Zhuoying Xie, Ligu Sun, Zhong-Ze Gu.** s.l. : Electroanalysis, 2009.
61. *Polymersome-Embedded Nanoparticles.* **Robert Sachsenhofer, Wolfgang H. Binder, Dominique Farnik, Ronald Zirbs.** s.l. : Macromol. Symp., 2007.
62. *Entrapment of Metal Nanoparticles in Polymer Stomatocytes.* **Daniela A. Wilson, Roeland J. M. Nolte, and Jan C. M. van Hest.** s.l. : JACS, 2012.
63. *Size Selective Incorporation of Gold Nanoparticles in Diblock Copolymer Vesicle Wall.* **Jiangping Xu, Yuanyuan Han, Jie Cui, and Wei Jiang.** s.l. : Langmuir, 2013.
64. *Biodegradable Theranostic Plasmonic Vesicles of Amphiphilic Gold Nanorods.* **Jibin Song, Lu Pu, Jiajing Zhou, Bo Duan, and Hongwei Duan.** s.l. : ACS Nano, 2013.
65. *Self-assembly of polystyrene with pendant hydrophilic gold nanoparticles: the influence of the hydrophilicity of the hybrid polymers.* **Jia Tian, Fan Zheng, Qingjiao Duan and Hanying Zhao.** s.l. : J. Mater. Chem, 2011.
66. *Synthesis, Stability, and Cellular Internalization of Gold Nanoparticles Containing Mixed Peptide-Poly(ethylene glycol) Monolayers.* **Yanli Liu, Mathew K. Shipton, Joseph Ryan, Eric D. Kaufman, Stefan Franzen, and Daniel L. Feldheim.** s.l. : Anal. Chem., 2007.
67. *Preparation and structures of supramolecules between cyclodextrins and polymers.* **Harada, Akira.** s.l. : Coordination Chemistry Reviews, 1996.
68. *Host-Guest Complexation Studied by Fluorescence Correlation Spectroscopy: Adamantane-Cyclodextrin Inclusion.* **Daniel Granadero, Jorge Bordello, Maria Jesus Pérez-Alvite, Mercedes Novo and Wajih Al-Soufi.** s.l. : Int. J. Mol. Sci., 2010.

69. *Biocompatible vesicles based on PEO-b-PMPC/ α -cyclodextrin inclusion complexes for drug delivery.* Gongyan Liu, Qiao Jin, Xiangsheng Liu, Liping Lv, Chaojian Chen and Jian Ji. s.l. : Soft Matter, 2010.
70. *Cyclodextrin-Adamantane Host-Guest Interactions on the Surface of Biocompatible Adamantyl-Modified Glycodendrimers.* Marco Paolino, Franka Ennen, Stefania Lamponi, Mihaela Cernescu, Brigitte Voit, Andrea Cappelli, Dietmar Appelhans, and Hartmut Komber. s.l. : Macromolecules, 2013.
71. *Cyclodextrin and Adamantane Host-Guest Interactions of Modified Hyperbranched Poly(ethylene imine) as Mimetics for Biological Membranes.* s.l. : Angew. Chem. Int. Ed., 2011.
72. *Vesicular gold assemblies based on host-guest inclusion and its controllable release of doxorubicin.* Wei Ha, Yang Kang, Shu-Lin Peng, Li-Sheng Ding, Sheng Zhang and Bang-Jing Li. s.l. : Nanotechnology, 2013.
73. *Self-Assembled Monolayers of Thiolates on Metals as a Form of Nanotechnology.* J. Christopher Love, Lara A. Estroff, Jennah K. Kriebel, Ralph G. Nuzzo, and George M. Whitesides. s.l. : Chem. Rev., 2005.
74. *pH-Dependent Release of Doxorubicin from Fast Photo-Cross-Linkable Polymersomes Based on Benzophenone Units.* Mohamed A. Yassin, Dietmar Appelhans, Rafael G. Mendes, Mark H. Rummeli, and Brigitte Voit. s.l. : Chem. Eur. J., 2012.
75. *Self-Assembly of Amphiphilic Plasmonic Micelle-Like Nanoparticles in Selective Solvents.* Jie He, †, # Xinglu Huang, Yan-Chun Li, || Yijing Liu, Taarika Babu, Maria A. Aronova, Shouju Wang, Zhongyuan Lu, Xiaoyuan Chen, and Zhihong Nie. 2013, Journal of the American Chemical Society.
76. *Synthesis, Stability, and Cellular Internalization of Gold Nanoparticles Containing Mixed Peptide-Poly(ethylene glycol) Monolayers.* Yanli Liu, Mathew K. Shipton, Joseph Ryan, Eric D. Kaufman, Stefan Franzen and Daniel L. Feldheim. 2007, Analytical Chemistry.
77. *Preparation of Functionally PEGylated Gold Nanoparticles with Narrow Distribution through Autoreduction of Auric Cation by r-Biotinyl-PEG-block-[poly(2(N,N dimethylamino)ethyl methacrylate)].* Takehiko Ishii, Hidenori Otsuka, Kazunori Kataoka, and Yukio Nagasaki. s.l. : Langmuir, 2004.
78. *Size Correlation of Optical and Spectroscopic Properties for Gold Nanoparticles.* Peter N. Njoki, I-Im S. Lim, Derrick Mott, Hye-Young Park, † Bilal Khan, Suprav Mishra, Ravishanker Sujakumar, Jin Luo, and Chuan-Jian Zhong. s.l. : The Journal of Physical Chemistry C, 2007.
79. *Vesicular gold assemblies based on host-guest inclusion and its controllable release of doxorubicin.* Wei Ha, Yang Kang, Shu-Lin Peng, Li-Sheng Ding, Sheng Zhang and Bang-Jing Li. s.l. : Nanotechnology, 2013.
80. *Multivalent Aggregation of Cyclodextrin Gold Nanoparticles and Adamantyl-Terminated Guest Molecules.* Olga Crespo-Biel, Amela Jukovic, Maria Karlsson, David N. Reinhoudt, and Jurriaan Huskens. s.l. : Israel Journal of Chemistry, 2004.
81. *Incorporation of Nanoparticles into Polymersomes: Size and Concentration Effects.* Karmena Jaskiewicz, Antje Larsen, David Schaeffel, Kaloian Koynov, Ingo Lieberwirth, George Fytas, Katharina Landfester, and Anja Kroeger. s.l. : ACS Nano, 2012.

82. *In Situ Formation of Gold-“Decorated” Vesicles from a RAFT-Synthesized, Thermally Responsive Block Copolymer.* **Yuting Li, Adam E. Smith, Brad S. Lokitz, and Charles L. McCormick.** s.l. : Macromolecules, 2007.

83. *Polymersome-Embedded Nanoparticles.* **Robert Sachsenhofer, Wolfgang H. Binder, Dominique Farnik, Ronald Zirbs.** s.l. : Macromolecule Symposium, 2007.

84. *pH-Sensitive Vesicles Based on a Biocompatible Zwitterionic Diblock Copolymer.* **Jianzhong Du, Yiqing Tang, Andrew L. Lewis, and Steven P. Armes.** s.l. : Journal of the American Chemical Society, 2005.

85. *Self-Assembly of Amphiphilic Plasmonic Micelle-Like Nanoparticles in Selective Solvents.* **Jie He, Xinglu Huang, Yan-Chun Li, Yijing Liu, Taarika Babu, Maria A. Aronova, Shouju Wang, Zhongyuan Lu, Xiaoyuan Chen, and Zhihong Nie.** s.l. : Journal of the American Chemical Society, 2013.

86. *Preparation of liposomes of defined size distribution by extrusion through polycarbonate membranes.* **F. Olson, C. A. Hunt, F. C. Szoka, W. J. Vail and D. Papahadjopoulos.** s.l. : Biochimica et Biophysica Acta, 1979.

